MDOT STATE STUDY #269 - Driven Pile Load Test Data Analysis and Calibration of LRFD Resistance Factor for Mississippi Soils

A Final Report Submitted by:

Eric J. Steward, Ph. D., P.E.
Associate Professor, Department of Civil, Coastal, & Environmental Engineering
University of South Alabama
Mobile, AL 36688
esteward@southalabama.edu
251-460-6174

Co-Authored by Graduate Students:
Axel Arnold Yarahuaman Chamorro
Dianabel Jackeline Giron Gonzalez

December 2020

FHWA Technical Report Documentation Page

1. Report No. FHWA/MDOT-RD-20-269	2. **Government Accession No.**	**3. Recipient's Catalog No.**
4. Title and Subtitle Driven pile load test data analysis and calibration of LRFD Resistance factor for Mississippi soils		**5. Report Date** December 22, 2020 **6. Performing Organization Code**
7. Author(s) *Eric Steward*, Ph.D. PE (ORCID: 0000-0002-1714-740X) *Dianabel Giron Gonzalez* *Axel Yarahuaman*		**8. Performing Organization Report**
9. Performing Organization Name and Address University of South Alabama Department of Civil, Coastal, & Environmental Engineering 150 Student Services Drive Mobile, AL 36688		**10. Work Unit No. (TRAIS)** **11. Contract or Grant No.**
12. Sponsoring Agency Name and Address Mississippi Department of Transportation Research Division 86-01 PO Box 1850 Jacksion, MS 39215-1850		**13. Type Report and Period Covered** January 2017 to December 2020 **14. Sponsoring Agency Code**
15. Supplementary Notes		

16. Abstract

The Mississippi Department of Transportation (MDOT) currently uses LRFD. However, the LRFD resistance factor used does not necessarily represent the Mississippi soils. A pair of authors have already calibrated LRFD resistance factors for other states using First Order Second Moment (FOSM). However, FOSM leads to over-conservatism. Thus, this study calibrated LRFD resistance factors using the First Order Reliability Method and Monte Carlo Simulation (MCS) rather than FOSM. MCS was found to be the most efficient method. Moreover, pile setup factors were obtained in different sets of data. Finally, the calibrated resistance factors were compared with the recommended resistance factors from published studies from the federal government and the state of Alabama in terms of accuracy. The resistance factors generated in this study are recommended for use based on MDOT's design methodology.

17. Key Words Pile Design, LRFD, Pile Setup		**18. Distribution Statement**	
19. Security Classif. (of this report) Unclassified	**20. Security Classif. (of this page)** Unclassified	**21. No. of Pages** 73	**22. Price**

DISCLAIMER

The University of South Alabama and the Mississippi Department of Transportation do not endorse service providers, products, or manufacturers. Trade names or manufacturers' names appear herein solely because they are considered essential to the purpose of this report.
The contents of this report do not necessarily reflect the views and policies of the sponsor agency.

MDOT – STATEMENT OF NONDISCRIMINATION

The Mississippi Department of Transportation (MDOT) operates its programs and services without regard to race, color, national origin, sex, age or disability in accordance with Title VI of the Civil Rights Act of 1964, as amended and related statutes and implementing authorities.

MISSION STATEMENTS

The Mississippi Department of Transportation (MDOT)

MDOT is responsible for providing a safe intermodal transportation network that is planned, designed, constructed and maintained in an effective, cost efficient and environmentally sensitive manner.

The Research Division

MDOT Research Division supports MDOT's mission by administering Mississippi's State Planning and Research (SP&R) Part II funds in an innovative, ethical, accountable, and efficient manner, including selecting and monitoring research projects that solve agency problems, move MDOT forward, and improve the network for the traveling public.

AUTHOR ACKNOWLEDGMENTS

The authors wish to thank to the Mississippi Department of Transportation for sponsoring this research, especially, Sean Ferguson and Michael Stroud in the Geotechnical Engineering department.

TABLE OF CONTENTS

Page

LIST OF TABLES

Page

LIST OF FIGURES

Page

LIST OF ABBREVIATIONS

COV_Q	Coefficient of variation of loads or coefficient of variation of the bias values for the loads.
COV_{QD}	Coefficient of variation of dead load or coefficient of variation of the bias values for the dead load.
COV_{QL}	Coefficient of variation of live load or coefficient of variation of the bias values for the live load.
COV_R	Coefficient of variation of the resistance or coefficient of variation of the bias values for the resistance.
G	Limit state equation function
g_i	Limit state function of value i
n	Number of failures
N	Number of simulations for Monte Carlo simulation.
NORMSINV	A Microsoft Excel function that returns the inverse of the standard normal distribution.
$P_{f\,true}$	True probability of failure
P_f:	Probability of failure
q^*	Trial Load standard normal space design point
Q	Load random variable
q	Standard normal space design point for the load
q_D	Predicted (nominal) value of dead load.
QD_i, $\lambda_{QD,i}$	Simulated dead load value i
Q_i, $\lambda_{Q,I}$	Simulated load value i
q_L	Predicted (nominal) value of live load.
QL_i, $\lambda_{QL,I}$	Simulated live load value i
Q_n	Nominal load.
r^*	Trial Resistance standard normal space design point
R	Resistance random variable
r	Standard normal space design point for the resistance.
R_{EOID}	Nominal EOID resistance.

R_i, $\lambda_{R,I}$	Simulated resistance value i
r_n, R_n	Nominal resistance
R_{setup}	Nominal setup resistance increase
V_p	Coefficient of variation of the estimated probability established
β	Reliability index
β_T	Target reliability index.
γ_{avg}	Average load factor
γ_Q	Load factor for loads.
γ_{QD}	Load factor for dead load.
γ_{QL}	Load factor for live load.
η	Dead-to-live ratio (Q_D/Q_L)
λ_Q	Normal mean of the bias values for the loads.
λ_{QD}	Normal mean of the bias values for the dead load.
λ_{QL}	Normal mean of the bias values for the live load.
λ_R	Normal mean of the bias values for the resistance.
σ_Q	Standard deviation for the load Q or the measured load $Q_{measured}$.
σ_{QN}	The normal standard deviation for the load Q.
σ_R	Standard deviation for the resistance R or the measured resistance $R_{measured}$.
$\sigma_{\lambda D}$	Standard deviation of the dead load dataset.
$\sigma_{\lambda L}$	Standard deviation of the live load dataset.
$\sigma_{\lambda R}$	Standard deviation of the resistance dataset.
ϕ_{EOID}	Resistance Factor for EOID nominal resistance
ϕ_R,ϕ	Resistance Factor
ϕ_R/λ	Bias Efficiency factor
ϕ_{setup}	Resistance Factor for setup nominal resistance.

EXECUTIVE SUMMARY

In 2007, the American Association of State Highway and Transportation Officials (AASHTO) published a new policy requiring the application of the Load and Resistance Factor Design (LRFD) methodology for pile foundations. The Mississippi Department of Transportation (MDOT) currently uses LRFD. However, the LRFD resistance factor used does not necessarily represent the Mississippi soils. A pair of authors have already calibrated LRFD resistance factors for other states using First Order Second Moment (FOSM). However, FOSM leads to over-conservatism. Thus, this study calibrated LRFD resistance factors using the First Order Reliability Method and Monte Carlo Simulation (MCS) rather than FOSM. MCS was found to be the most efficient method. Moreover, pile setup factors were obtained in different sets of data. Finally, the calibrated resistance factors were compared with the recommended resistance factors from published studies from the federal government and the state of Alabama in terms of accuracy. The resistance factors generated in this study are recommended for use based on MDOT's design methodology.

CHAPTER I – INTRODUCTION

Pile foundations are used extensively as support for high-rise buildings, bridges and other heavy structures, and to safely transfer the structural loads and moments to the ground. Piles are also used to avoid excess settlement or lateral movement. Piles are designed to carry the structural loads and maintain construction costs as low as possible at the same time. Nevertheless, the design of pile foundations involves a significant number of uncertainties which can be translated generally to over-conservatism. One way to decrease the construction costs is to develop more accurate prediction methods through static analysis methods, design programs, dynamic analysis methods, and pile setup consideration. If the anticipated pile resistance is more accurately estimated before driving, pile lengths and sizes can be reduced and, hence, cost savings are achieved. Therefore, it is clear that managing uncertainty is largely important to use resources, time, and money efficiently.

The basic pile design starts with static analysis methods or design programs. Both are related since design programs incorporate one or more static analysis methods to estimate the pile capacity. The static analysis methods allow engineers to estimate the pile length and pile size prior to installation. Several static analysis methods are available and each one of them has specific applications, limitations, and soil parameters required. In the same way, several design programs have become more popular due to their time efficiency, and they use these static analysis methods to determine the estimate capacity of the pile at specific locations. These programs include DrivenPile and APile, which are available commercially.

Once the pile length, pile size, and nominal resistance are estimated through static analysis methods or design programs, the designs are confirmed during construction by field control determination tests or methods. The most accurate method to verify the pile capacity is through static load testing. Static load tests consist of loading the pile using a load cell attached to a reaction system that keeps the load cell fixed. The load increases gradually until failure. Another method used to verify or revise design is through dynamic load testing based on dynamic analysis and wave propagation theory. Dynamic tests consist of a hammer hitting the head of a pile during and after installation. The compression wave data during hammer blows is obtained and processed through a Pile Driving Analyzer (PDA*),* which can incorporate signal

matching (CAPWAP). Dynamic load testing can be considered as an economically efficient method to determine the capacity of a pile compared to the significant cost of static load testing.

Another aspect of design capable of producing cost-savings for pile design is the phenomenon known as pile setup, which consists of a pile resistance or capacity increase over some time interval after installation. When the pile is being driven, the surrounding soil is disturbed and loses strength. Once the installation has finished, the same soil starts a process to attempt to recover lost strength, which contributes to an increase in the pile capacity. If the pile capacity increase is accurately anticipated, the pile length, sizes and quantity can be decreased, hence lower costs would be required. Pile setup capacity increase can be measured immediately or some time interval after installation through dynamic load tests. Several prediction models to predict this capacity increase are available, but the most popular is the Skov and Denver [1] model.

Driven piles have been designed following the Allowable Stress Design (ASD) methodology for years. ASD represents the construction uncertainties and safety margin typically through a single factor of safety (FS). For ASD, the pile capacity is reduced by dividing the nominal pile capacity by the FS. Nonetheless, the limitations of ASD were recognized in the 1990s [2]. Consequently, an alternative design methodology known as Load and Resistance Factor Design (LRFD) has been developed since the mid-1980 [3] and is becoming more popular due its reliability basis. For LRFD, loads and resistance have different sources and levels of uncertainty. Thus, each one (loads and resistances) is modified by partial factors. The loads are affected by load factors that are larger or equal to 1. The resistance is affected by resistance factors that are smaller or equal to 1. In other words, if LRFD is employed, the loads are amplified while the resistance is underestimated. In this way, LRFD generates a design with more consistency and uniform level of safety [2]. Consequently, more economically efficient and repeatable designs are possible compared to ASD methodology [3].

Under LRFD, the resistance is reduced by multiplying the nominal capacity by a resistance factor (ϕ). This resistance factor can be lower or equal to 1 and can be calibrated for a specified regional soil if enough statistical data is available. The calibration depends on significant data sizes and is based on probability theory. The most widely used probability-based methods to calibrate a resistance factor are the First Order Second Method (FOSM), the First Order Reliability Method (FORM), and Monte Carlo Simulation (MCS). The three methods

require a resistance bias factor (λ_R) obtained from the ratio between a set of measured capacity data and a set of predicted capacity data. The measured capacity is obtained from field test such as dynamic and static load testing, while the predicted capacity is obtained from static analysis method or design programs.

Overthe past few decades, several efforts have been made to implement and develop LRFD resistance factors for deep foundations for bridges. Nonetheless, the transition has been relatively slow [4] due to the large quantity and quality of data required, as well as deficiencies included in the early development of LRFD specifications. The American Association of State Highway and Transportation Officials (AASHTO) and the Federal Highway Administration (FHWA) published a policy that turned into an obligation for the usage of LRFD for all new bridges initiated after October 1st, 2007. Therefore, AASHTO also provided some recommended resistance factors for various design methods along with the policy. Nevertheless, several Departments of Transportation (DOTs) expressed their concern about the accuracy and over-conservatism of these resistance factors when applied to specific regions [3]. Consequently, AASHTO and FHWA allowed the state Department of Transportations to develop their regionally calibrated LRFD resistance factors for bridge foundations incorporating statistical and reliability theory using existing databases. Since then, several DOTs started working on the composition of adequate databases and the development of their own LRFD resistance factors to eliminate over-conservative designs and generate cost savings to the state and taxpayers.

Studies conducted by NCHRP 507 [5], Styler [6], Haque and Abu-Farsakh [7] revealed that FOSM tends to lead to some over-conservatism. For instance, NCHRP 507 [5] found that FOSM provides resistance factors 10% lower than FORM. Moreover, Styler [6] contends that FORM resistance factors tend to be 8%-23% larger than FOSM resistance factors. Also, Allen et al. [8] suggests that MCS is more adaptable and rigorous method than FOSM and provides resistance factors consistent with FORM. Consequently, the main objective of this study is to develop LRFD resistance factors unique to Mississippi soils using FOSM, FORM, and MCS, in order to enhance accuracy and efficiency of pile design. The second objective is to develop pile setup factors in different sets of data. Finally, the third objective is to compare the calibrated resistance factors with the recommended resistance factors from published studies.

CHAPTER II – LITERATURE REVIEW

This chapter describes and explains the basic concepts and background information applied to the subsequent chapters of this study. The main conceptual sections included are (1) driven piles, (2) basic pile design, (3) ASD methodology, (4) LRFD methodology, (5) pile load testing, and (6) pile setup. Some sentences, tables, figures, graphs, and equations will be referenced in the following chapters of the study.

2.1 Driven Piles

The first problem for a foundation designer is to establish whether the soil conditions are suitable to support the structure using shallow foundations or deep foundations (such us piles). Vesic [9] says that "piles are used where upper soil strata are compressible or weak; where footings cannot transmit inclined, horizontal, or uplift forces; where scour is likely to occur; where future excavation may be adjacent to the structure; and where expansive collapsible soils extend for a considerable depth". The FHWA [10] adds that pile foundations are used extensively to support buildings, bridges, and other heavy structures, to safely transfer structural loads to the ground, and to avoid excess settlement or lateral movement. According to Pement [2], driven piles and drilled shaft are the most common deep foundations.

Driven piles can be installed by impact driving or vibrating. There are two types of driven piles: End-bearing piles and friction piles. On one hand, End-bearing piles resist loads through the interaction of the cross-sectional area of its tip and the hard layer beneath. Although a minimal friction resistance is developed, this is usually ignored. On the other hand, friction piles resist loads through the interaction and friction of the perimetrical pile area and the soil around it. When bedrock is not encountered at a reasonable depth below the ground surface, piles can resist loads through both end-bearing and frictional resistance for economic efficiency [2].

2.2 Basic Pile Design

One of the most important challenges for foundation engineering, especially for pile design, is to develop a safe and cost-effective foundation system. National committees such as the FHWA, American Concrete Institute (ACI), American Institute of Steel Construction (AISC), and the AASHTO are deeply involved in the updating of design requirements. However, in the geotechnical field, several variables affect the soil conditions and its interaction with a structure. Therefore, *the soil conditions can be estimated, but cannot be determined with complete accuracy* [2]. Generally, the required capacity and depth shall be estimated before driving the pile. Thus, it is vital to predict the amount of nominal resistance of the pile with a reasonable accuracy despite the complex nature of the soils. This prediction or design can be performed through static analysis or design programs, which can implement several design methods.

2.2.1 Software Program Analysis

Due to its time efficiency, software program analysis is becoming more popular for engineering purposes. As indicated by Pement [2], Software Program Analysis are mainly used for axial loaded single piles or pile groups. These programs can include one or several static analysis design methods. Also, they incorporate different soil layers, soil types, soil characteristics, which are used to estimate the pile capacity according to a specific depth. Table 1 summarizes some of the available commercial programs including the static analysis programs that they are based on.

Table 1. Summary of Computer Analysis Software for Axial Single Pile Analysis (FHWA, 2016).

Computer Program	Static Analysis Methods In Program	Method Presented in GEC-12 (2016)	Method Presented in AASHTO 7th edition (2014)
AllPile	Navfac DM-7	No	No
A-Pile	API-RP2A	Yes	No
A-Pile	US Army COE	No	No

A-Pile	FHWA (Alpha / Nordlund)	Yes	Yes
A-Pile	Lambda Method	No	Yes
A-Pile	NGI (CPT)	No	No
A-Pile	ICP (CPT)	No	No
DrivenPiles	Alpha Method	Yes	Yes
DrivenPiles	Nordlund Method	Yes	Yes
FB-Deep	FDOT SPT Method	No	No
FB-Deep	Schmertmann (CPT)	Yes	Yes
FB-Deep	UF (CPT)	No	No
FB-Deep	LCPC (CPT)	No	No
Unipile	Alpha Method	Yes	Yes
Unipile	Beta Method	Yes	Yes, but differs
Unipile	Elsame and Fellenious (CPT)	Yes	No
Unipile	Schmertmann (CPT)	Yes	Yes
Unipile	LCPC (CPT)	No	No
Unipile	Meyerhof (SPT)	No	Yes

2.2.2 APile

The computer software currently used by the Mississippi Department of Transportation (MDOT) to design pile foundations is APile. The program utilizes four different methods for computations of pile capacity as a function of the encountered soil properties and the type of material used for the pile. The methods used for computations are American Petroleum Institute (API RP-2A), U.S. Army Corps of Engineers (USACE), Federal Highway Administration (FHWA), and Revised Lambda Method.

Pile load-carrying capacity depends on various factors. Two widely used methods for pile design will be described, the alpha method (α) –used to calculate the short-term load capacity (total stress) of piles in cohesive soils, and beta method (β) –used to calculate the long-term load capacity (effective stress) of piles in both cohesive and cohesionless soils [11].

The Alpha (α) method is the most common method of calculating the capacity for skin friction of driven piles in cohesive soils. The skin friction as compared to the undrained shear force with empirical coefficients named α in the field load test results. Total stress is the total tension per unit area of the surface, which is the sum of the positive and unfavorable stresses.

The beta method (β) allows the engineer to calculate the vertical bearing capacity of a separate pile in both cohesive and non-cohesive soils. By obtaining total stress and pore water pressures information, effective stress can be measure. The method is based on effective stress analysis and is suited for long-term (drained) analyses of pile load capacity [11]. Also, regular stresses and just not shear stresses are defined by the concept of effective stress. Soil deformation is a vital stress mechanism, not an overall tension.

2.3 Allowable Stress Design (ASD) Method

ASD design methodology has been used for decades in the Geotechnical engineering field as a way to incorporate uncertainties into a design. This method consists of utilizing a limit equilibrium analysis by keeping the anticipated loads lower than the capacity or resistances. In ASD, the uncertainties in the loads and resistances are expressed in an incorporated value named "Factor of Safety" (FS). Pement [2] suggests that the uncertainties from a design method are most likely due to (1) variability of engineering properties and load predictions, (2) errors in measuring material resistance, (3) errors in prediction models used, and (4) sufficiency and applicability of sampling and testing methods. The ASD design equation used is the following:

$$\frac{R_n}{FS} \geq \sum Q_i \tag{1}$$

where R_n is the nominal resistance (capacity), FS is the Factor of Safety, and $\sum Q_i$ is the sum of load effects (dead, live, and environmental) applied on a pile [12].

Nevertheless, ASD is becoming less popular due to the following limitations. (1) The Factor of Safety (FS) is a subjective value that is not based of probability of failure. The FS just depends on the design models and material parameters selected [2]. (2) ASD assumes similar uncertainties for load and resistance variables. (3) ASD is based only on experience and engineering judgment, which can lead to over conservatism [12]. Even though several sources of uncertainties can be considered by the designer when using ASD, their consideration is mainly qualitative rather than quantitative [13].

Figure 1 shows the way ASD reduces the probability of failure when probability density functions are evaluated. Failure is defined as loads exceeding the resistance, which graphically represented by the area formed by the load curve overlapping the resistance curve. The graph on the left shows when load and resistance are unmodified, hence, they are similar theoretically. The graph on the right shows when the resistance has been modified by the FS. The displacement of the resistance probability density function curve, due to the FS, reduces the probability of failure by decreasing the overlapped area. The new failure area is represented in orange color.

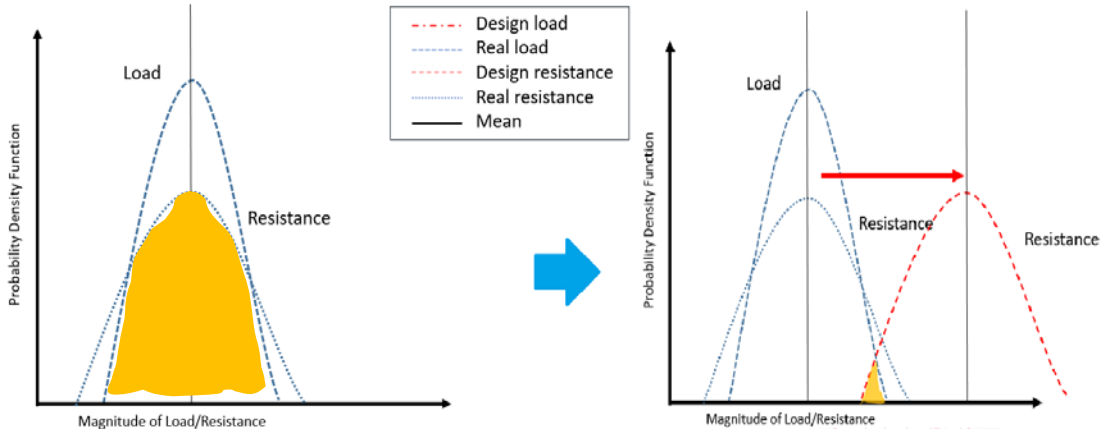

Figure 1: Probability density function for load and resistance when ASD is used (Cleary, 2019).

2.4 Load and Resistance Factor Design (LRFD) Method

Load and Resistance Factor Design (LRFD) is an alternative design methodology specifically and progressively developed for bridges since the mid-1980s [3]. LRFD originated due to the limitations of ASD methodology recognized in the 1990s [2]. Moreover, AASHTO required the LRFD method to design deep foundations supporting bridges in 2007. The LRFD design equation is the following:

$$\phi R_n \geq \sum \gamma_i Q_i, \tag{2}$$

where ϕ is the resistance factor, R_n is the nominal resistance or capacity, γ_i is the load factor, Q_i is the nominal load value.

Under LRFD, both loads and resistance have different sources and levels of uncertainty. These uncertainties can be quantified using probability-based procedures to satisfy engineered design with consistent and specific levels of reliability. Paikowsky et al. [5] says that "The principal difference between Reliability Based Design and the traditional or partial factors of safety design approaches lies in the application of reliability theory, which allows uncertainties to be quantified and manipulated consistently in a manner that is free from self-contradiction." In other words, the implementation of LRFD allows the separation of uncertainties from loads and resistances and, then, to use methods based on probability theory to satisfy a prescribed margin of safety [5]. It should be noted that since loads are better known than resistances, the load effect usually has smaller variability than the resistance effect.

Figure 2 shows the way LRFD reduces the probability of failure when probability density functions are evaluated. Failure is defined as loads exceeding the resistance. This failure is graphically translated to point where the load curve overlaps the resistance curve. The graph on the left shows when load and resistance are unmodified, hence, they are similar theoretically. The graph on the right shows when the loads have been factored (increased) by the load factors and the resistance has been factored (decreased) by the resistance factor. The displacement of the load and resistance probability density function curve to opposite directions reduces the probability of failure by decreasing the overlapped area. The new failure area is represented in orange color.

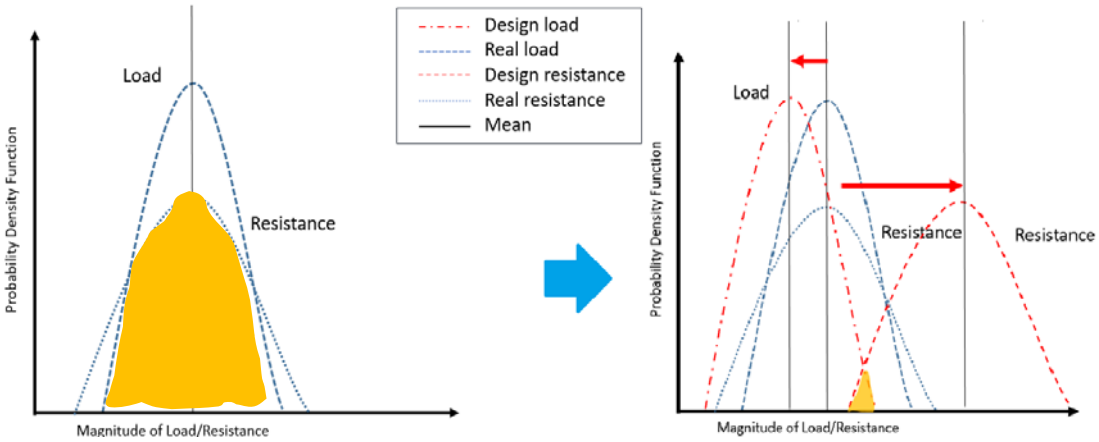

Figure 2: Probability density function for load and resistance when LRFD is used (Cleary, 2019).

As mentioned by Paikowsky et al [5], some of the specific benefits of implementing LRFD for pile design include the following:

- Cost savings and improved reliability due to more efficiently balanced design.
- More rational and rigorous treatment of uncertainties in the design.
- Enhanced perspective on the overall design and construction processes.
- Development of probability-based design method capable of stimulating advances in pile analysis and design.
- Conversion of the codes into living and easier to revise documents.
- The factors of safety previously used provide a framework to extrapolate existing design procedures into newer foundation concepts and materials.

Currently the Mississippi DOT utilizes LRFD in the design methodology of driving piles by incorporating the resistance factors developed from the national database as generated by the AASHTO Design Manual [14]. However, utilizing regionally calibrated resistance factors are recommended and preferred to increase the accuracy of the predicted capacity of driven piles.

2.5 Pile Axial Load Test

Load testing is the most accurate way to determine the nominal capacity of a pile [2]. Due to the high uncertainty of soils involve, it is imperative to perform actual load tests before or during construction to verify the preliminary design. The load tests are best known as field control methods. AASHTO states that when nominal axial resistance is determined by using actual load testing, the uncertainty in the nominal axial resistance is solely due to the reliability of the field determination method. They are mainly classified into two axial field control methods: Static Load Test (SLT) and Dynamic Load Test (DLT).

2.5.1 Static Load Test

Load tests are commonly conducted to determine a pile foundations' capability to sustain working loads while offering the right level of safety. Due to the non-availability of established procedures of assessing mechanisms of transferring loads between the soil and the piles, load tests are conducted, usually during the design or construction phase [15]. Static Load Test is the most accurate method to determine the pile load capacity.

FHWA [16] says that “depending upon the size of the project and other project variables, static load tests may be performed either during the design stage or construction stage.” Usually, a SLT is performed inside or close to the site of the final pile installation. Once a pile is installed, a waiting period is required before the pile can be tested.

The axial Static Load Test is regulated by ASTM D 1143-07 [17]. A system of reaction beams is attached to the load cell to assure minimum displacement as shown in Figure 3 Generally, the reaction beams are connected to reaction piles. ASTM D 1143-07 [17] mentions several loading methods. However, the Quick Maintained (QM) Testing Method is the fastest and most efficient when determining the pile capacity [18]. In this method, the load is applied in increments of 5% of the anticipated nominal resistance. Load can be incremented until pile failure. The load gradient shall be composed by at least 20 points before reaching the geotechnical nominal resistance in order to generate a load-displacement curve [2]. The test shall not last more than one hour as cited by Hannigan et al [19]. Once the load-displacement curve is plotted, several determination methods or acceptance criteria can be performed, such as the

Davisson Method, the Shape of Curvature Method, the Limited Total Settlement Method, the De Beer Method, the Chin methods, and the Iowa DOT method. However, the Davisson Method is the most popular method and works better with QM test data [20].

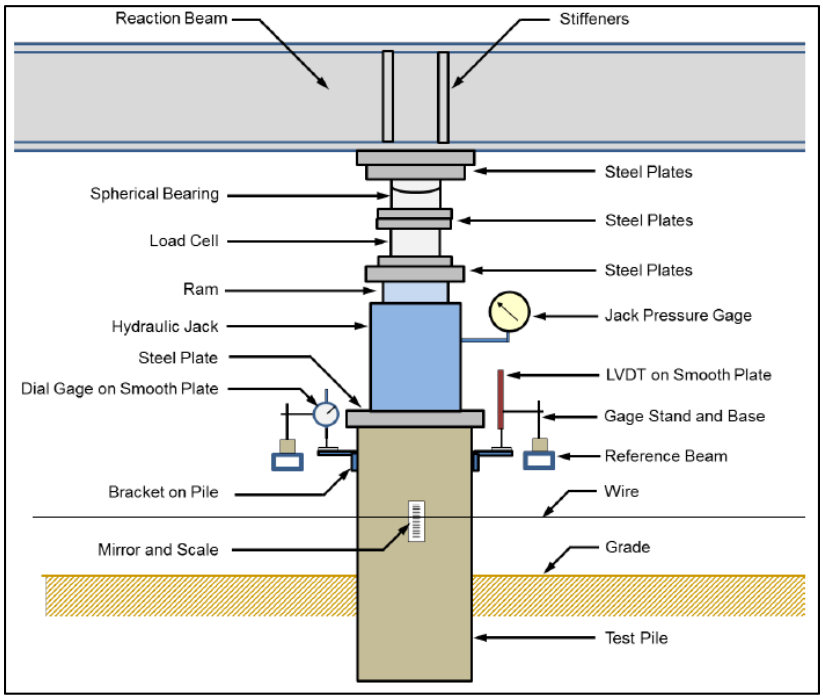

Figure 3: Static load test diagram (FHWA, 2016)

The Davisson Method is used to determine the load at which the pile fails and is based on the deformation of the pile head. It also uses a drawn line parallel to the elastic compression line (base line), which is offset by a specified amount of displacement depending on the pile size [18]. The parallel line is known as the Offset Limit Line or Davisson Line. According to Figure 4, the point of intersection between the Offset Limit Line and the load-displacement curve is considered the Nominal Resistance or Failure Load.

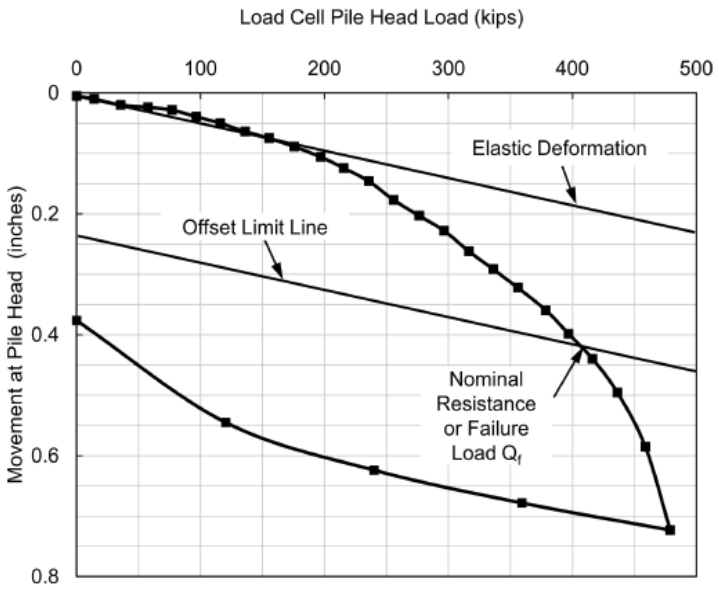

Figure 4: Load-Displacement Curve and The Davisson offset method (Hannigan et al, 2016)

The Elastic Deformation Line or Base Line can be plotted considering the following equation:

$$\Delta = \frac{Q_{va}L}{AE}, \tag{3}$$

where Δ is the elastic movement of the base line, Q_{va} is the applied load, A is the cross sectional are of the pile, E is the modulus of elasticity of the pile material, and L is the embedded length of the pile.

In addition, to draw the Offset Limit Line or Davisson Line, the following expression can be used:

$$X = 0.15 + \frac{D}{120}, \tag{4}$$

where X is the offset displacement from the base line (inches), and D is the pile diameter (inches).

With the application of a static load tester, engineers can obtain and record very reliable readings at various load intervals while monitoring various independent channels taken from

embedded sensors or the traditional pile top measurements [21]. The possibility of automatic data collection techniques allows engineers to monitor, analyze, and interpret the load test results in real-time. The method of pile load testing differs from other testing methods, such as dynamic and rapid load testing. The database used in this research project was obtained from dynamic tests. The Mississippi Department of Transportation did not perform static load tests in the tested piles that are used in this study.

2.5.2 Dynamic Load Test

Dynamic Load Testing is an economically efficient method to test a pile because the time involving the setup of testing equipment is low and simple. Dynamic Load Tests are performed typically during pile installation and a short time after the end of initial driving (EOID) and consists of obtaining compression wave data during hammer blows onto the pile head [2]. Basically, when the hammer strikes the top of the pile, a compressed stressed zone travels along the shaft of the pile at a constant wave speed. The speed depends mainly on the pile material. When the wave hits the pile toe, its amplitude is reduced by the action of static and dynamic soil resistance forces. Depending on the magnitude of the soil resistance, the wave will return to the top of the pile as a tensile (reflective) or compressive (incident) force [19]. Figure 5 shows the setup of the sensors in the crane and hammer system, while figure 6 shows this procedure of wave propagation.

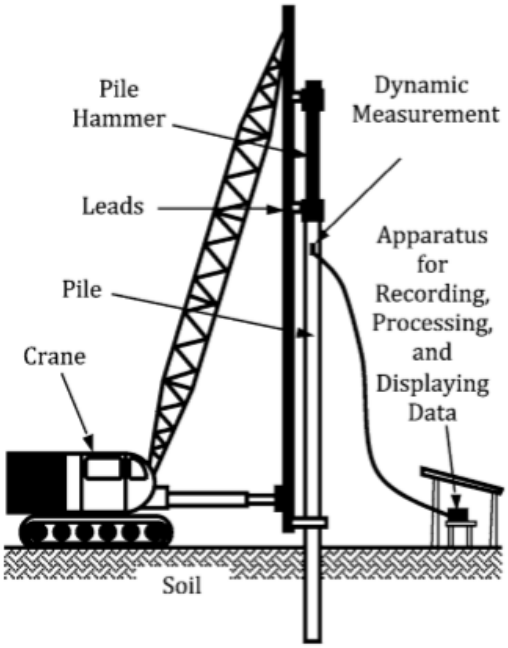

Figure 5: Typical setup of devices and gauges during dynamic testing (ASTM D4945-08).

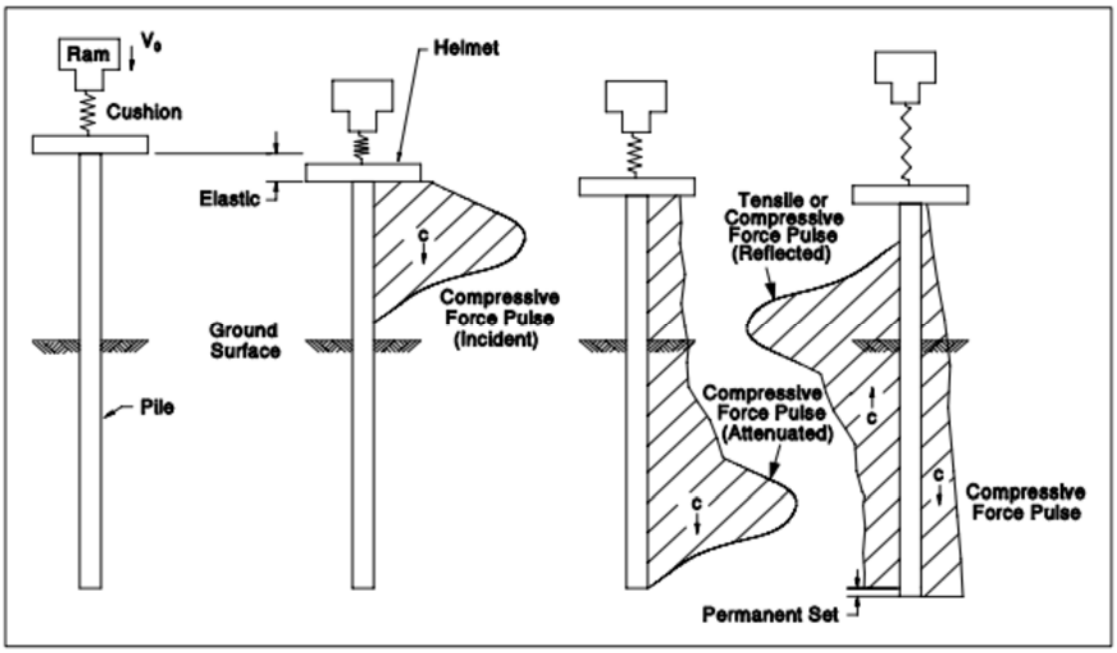

Figure 6: Wave propagation in a pile (Hannigan et al, 2016).

According to FHWA [16], Dynamic Load Tests use measurements of strain and acceleration taken near the pile head as a pile is driven or restrike with a pile driving hammer.

These dynamic measurements can be used to determine the performance of the pile driving system, calculate pile installation stresses, assess pile integrity, and evaluate the nominal geotechnical resistance [16]. However, Pement [2] says that when the pile is driven into the soil, the soil beneath behaves dynamically. Thus, it resists the pile in a dynamic manner. Consequently, it is not accurate to assume that the Dynamic resistance is equal to the Static resistance.

As mentioned by Pement [2], to perform a DLT, the pile has usually two or more transducers and accelerometer attached during pile installation. The gauges are connected to a computerized device called Pile Driving Analyzer (PDA), which receives the wave and energy data coming from the pile in real time. The PDA provides force and acceleration data, which is used to establish force and motion within the pile [2]. FHWA [16] adds that test results shall be better evaluated using signal matching techniques to determine the relative soil distribution on the pile and the dynamic soil properties to use in wave equation analyses.

There are several wave equations to determine the pile capacity such as dynamic formulas, wave equations, Case Pile Wave Analysis Program (CAPWAP), and iCAP. The last two methods are the most popular since they are programs that incorporate wave equations. Firstly, CAPWAP adopted the Smith [22] soil-pile model using the wave equation algorithm in the analysis to perform a signals-matching process with the combination of several analytical techniques [18]. CAPWAP basically partitions the pile into lumped masses linked with linear elastic springs and viscous dampers [18]. Second, iCAP is an automated version of CAPWAP designed to adjust for soil damping. Likins et al [23] mentions that iCAP results match very well with CAPWAP results for several types of piles and soils encountered.

The two ways to control the pile capacity through dynamic testing are through End of Initial Driving (EOID) and Beginning of Restrike (BOR). EOID is performed usually immediately after the pile has been installed and consists of restriking the pile head few times to get dynamic data. BOR analysis can be performed after one- or several-time intervals after EOID and requires few restrikes on the pile head as well. BOR is usually necessary when the pile capacity was not reached at EOID or past BOR tests. Dynamic Load Testing allows a comparison of EOID resistance and BOR resistance. In this way, setup can be quantified.

In summary, dynamic testing is based on wave propagation principles and uses wave equations to determine the nominal pile capacity. The most popular methods are CAPWAP and

ICAP, which are software that incorporate several wave equations. When static load tests are not available or performed, dynamic load tests are useful to perform EOID and BOR analysis and so it is possible to quantify the capacity of the pile at various times during and after the installation of the pile.

2.6 Pile Setup

Pile setup is defined as the pile capacity increase over time and might generate significant cost savings. Haque et al [7] defined pile setup as "the increase in axial resistance of driven piles after end of initial driving (EOID)." According to Haque and Steward [24], the incorporation of pile setup in the design stage would produce meaningful construction cost savings because the increase in pile capacity can translate into smaller pile elements or shorter embedment lengths. Pile setup phenomenon is mainly a product of three mechanisms: (1) Increase of soil effective stress due to the dissipation of excess pore water pressure, (2) thixotropic effect, and (3) stress independent increase or "aging" effect.

Firstly, during pile driving, the soil is displaced principally radially along the shaft and vertically below the toe. In the course of the driving process, the soil surrounding the pile loses strength due to an excessive increase of pore water pressure and distribution of soil pressure heavily disturbing the soil [25]. Immediately following EOID, this pore water excess begins to dissipate similarly to a consolidation process. Over time, the soil around the pile attempts to recover its original strength, which contributes to an increase in axial resistance of the pile [24]. Second, the phenomenon known was thixotropy also produces a regain of strength of the disturbed soil [26]. Thirdly, Schmertmann [27] indicates that even after the dissipation of excess pore water pressure is completed, pile setup can continue due to aging mechanism. Haque and Steward [24] state that aging effects increases the shear modulus, stiffness, dilatancy, friction angle of the soil and, also, reduces the soil's compressibility.

Several empirical models have been developed to predict pile setup behavior. However, the most popular is the one developed by Skov and Denver [1] due to its simplicity. This model uses the following equation:

$$\frac{R_t}{R_{to}} = A\, log_{10}\frac{t}{t_o} + 1, \tag{5}$$

where R_t is the total pile capacity at time t, R_{to} is the total pile capacity at reference time t_o, t is the time elapsed since end of initial pile driving, t_o is the initial reference time (usually time at EOID), and A is the setup parameter (log-linear).

The parameter A depends on the soil type, pile material, pile type, pile size, and pile capacity [24]. Skov and Denver [1] generally suggests using A = 0.2 for sand and A = 0.6 for clay.

The incorporation of setup into the calibration of LRFD resistance factors has been studied by Yang and Liang [28] and Haque et al. [7]. They take as basis the limit equation the same used by AASHTO [14], which does not incorporate setup:

$$\phi_R R_n = \gamma_{QD} q_D + \gamma_{QL} q_L, \quad (6)$$

where R_n is the predicted resistance, φ_R is the resistance factor for Rn, q_D and q_L are the predicted dead and live loads, respectively; and γ_{QD} and γ_{QL} are the load factors for q_D and q_L, respectively. In this way, Yang and Liang [28] proposes the setup effect of driven piles in the following equation:

$$\phi_{EOID} R_{EOID} + \phi_{setup} R_{setup} = \gamma_{QD} q_D + \gamma_{QL} q_L, \quad (7)$$

where φ_{EOID} and φ_{setup} are the resistance factors for reference resistance at t_{EOID} and setup resistance, respectively. R_{EOID} is the nominal resistance at end of initial driving, and R_{setup} is the nominal setup resistance increase.

Haque and Abu-Farsakh [7] evaluated the resistance factors for setup at time intervals of 30, 45, 60 and 90 days after EOID. Their final recommendation is using a setup resistance factor ϕ_{setup} of 0.35 at any time after the 14 days.

2.7 Research Purpose

The current MDOT state of practice for the LRFD design of driven piles is to utilize the generalized resistance factor (φ) as indicated by the AASHTO design manual [14]. The manual allows for regionally calibrated resistance factors with the appropriate amount of data gathered within the region. MDOT has tested thousands of piles over the past few decades, yet do not have a completed database to perform the necessary statistical analysis to calibrate the resistance factors for design.

Research has shown that driven piles experience up to 200% increase in axial resistance after installation, yet most design engineers neglect to include the effects of setup due to a lack of reliability and variable site conditions. Pile setup continues to occur beyond the standard 7 day restrike or load test time and if this long-term bearing capacity can be implemented into the pile design, the pile size or embedment depth can be reduced, resulting in considerably lower cost of a project. MDOT currently does not consider setup as a design parameter within the current state of practice, other than what the pile load tests indicate when the necessary resistances are not achieved during driving.

The study will develop a state wide pile load test database to then enable the development of a regionally calibrated LRFD resistance factor to improve the accuracy of driven pile design. The database will provide trends of pile setup in certain soil conditions within the state to then be included within the design parameters to improve the efficiency of the design of foundation elements of structures supporting MDOT bridges.

CHAPTER III – RESEARCH DATABASE AND METHODOLOGY

3.1 Research Database

The database used for the statistical evaluation of resistance factors for the design and construction of driven piles in Mississippi Soils was data obtained from MDOT consisting of PDA records, CAPWAP analyses, geotechnical reports, and the pile design recommendations. It was essential to organize the information obtained in an appropriate order that allowed a more efficient manipulation and evaluation of the database. A spreadsheet was composed of the information for 674 driven piles driven throughout the state of Mississippi. Figure 7 is a map of Mississippi with the location of each pile used in this study. The three types of piles driven within the state, Prestressed Concrete Piles (PSC), Steel H-Piles (HP), and Steel Pipe Piles (SPP), are shown in the figure as well.

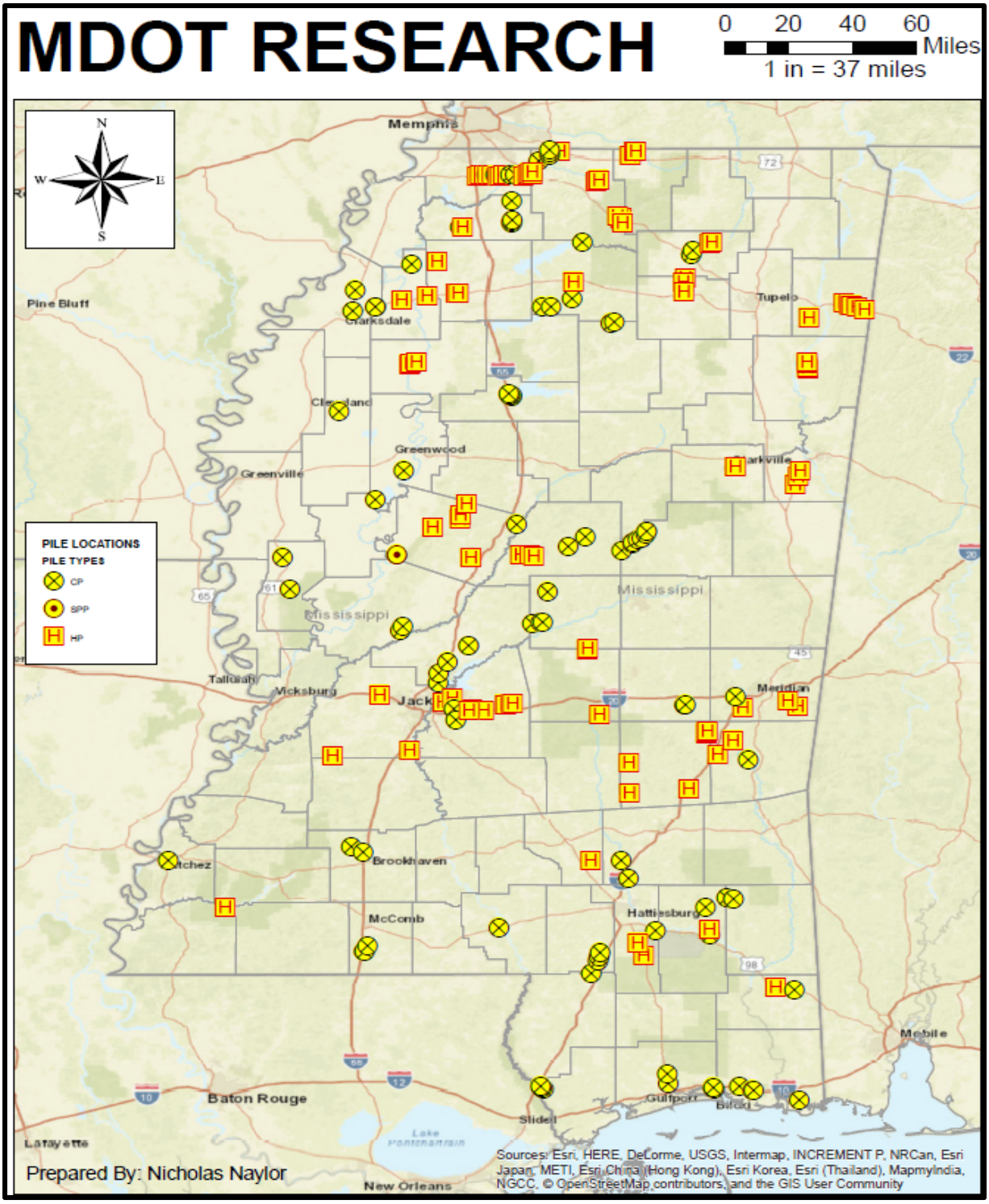

Figure 7: Location and type of piles used in this study in the State of Mississippi

3.2 Database Organization

It is generally suggested to organize the pile database into categories based on the pile material, soil type along the shaft, soil type beneath the toe, length, and geological regions. The piles in the database consisted of 283 PSC, 359 HP, and 22 SPP. Note that this is a total of 664 piles, as the type of material for 10 piles was unknown and the reports were unable to be obtained.

Geotechnical reports were used to determine the soil profiles encountered by each pile. The soil profile was simplified from many varying layers to either sand, clay, or mixed soil. Using the length of pile embedment, each pile was categorized by the type of soil encountered along the shaft and at the tip. The soil in contact with the pile's shaft was grouped to determine the majority of soil type providing friction resistance. The soil within the range of 10 feet above to 4 feet below the pile toe was used to determine the majority soil type providing the end bearing resistance. The depth of each soil layer type (sand or clay) along the embedment depth was added together, then taken as a percentage of the total embedment depth to find the majority soil type along the pile shaft. The majority of soil type was determined by applying a simple 35%-65% rule (See Equation 8). If the percentage of a soil type was greater than or equal to 65%, it was considered the majority, while the other 35% was disregarded. If neither type reached 65%, the profile stated as consisting of mixed soil.

$$Minority\ Soil\ Type \leq 35\% \leq Mixed\ Soil \leq 65\% \leq Majority\ Soil\ Type \qquad (8)$$

During the categorization of the behavior of the soil within these layers, it was observed that the silt encountered required additional analysis as some silts provided cohesive behavior while others did not. The silts with cohesive behavior were assumed to be clay, and cohesionless silts were assumed to be sand. After the soil profiles were created, each pile was provided a code number based on all of the possible soil types encountered. The list of soil profile scenarios between the shaft and tip layers can be seen in Table 2.

Table 2: List of the nine soil profiles encountered at each pile location

Soil Profile Code	1	2	3	4	5	6	7	8	9
Soil along the Shaft	Clay	Clay	Clay	Mixed	Mixed	Mixed	Sand	Sand	Sand
Soil at the Toe	Clay	Mixed	Sand	Clay	Mixed	Sand	Clay	Mixed	Sand

After a soil profile was determined and assigned to each pile, the four pile groups based on the material type previously presented were separated by their soil profile type. Each group was composed of nine subgroups, which is the soil profile code assigned. The number of piles in each subgroup is presented in Table 3. Soil profile code 9, which indicates the pile encounters mostly sand throughout its embedment length, is the most common soil type encountered. Note that 80 piles do not have a soil profile code assigned because there were no geotechnical reports provided, and 9 piles do not have material type information.

Table 3: Number of piles categorized by the pile material and soils encountered

Pile Material Type	Soil Profile Code									
	Total	**1**	**2**	**3**	**4**	**5**	**6**	**7**	**8**	**9**
ALL	593	106	19	45	54	31	116	20	12	190
PSC	242	41	5	26	25	17	48	8	9	63
HP	321	65	14	18	25	9	63	11	2	114
SPP	21	0	0	0	4	2	2	1	0	12

3.3 Driven Piles Database – Load Testing Data

The number of piles used for the statistical evaluation of resistance factors for the design and construction of driven piles in Mississippi Soils is different from the initial number of piles from the primary database due to missing information. Four different sets of data, shown in Tables 4, through 7, were used in the calibration of the resistance factors based on the level of detailed information utilized. Case A utilizes all piles only distinguished by the type of pile and the load test method. Case B only considers the soil profile code of each pile. Case C considered

the pile material first and then separated the database of each material into nine subgroups based on the soil profile code. While Case D considered five different subgroups based on a geologic map of Mississippi. Figure 8 is the geologic map that was used to categorize the different subgroups presented in Case D.

Table 4: Detailed Set of Data for Case A

Prediction Method	Measured Method	Data set A	Number of Piles
APILE	CAPWAP	All Piles	648
		PSC	279
		HP	347
		SPP	22
APILE	PDA	All Piles	652
		PSC	280
		HP	350
		SPP	22

Table 5: Detailed Data Set for Case B

Prediction Method	Measured Method	Data set B		Number of Piles
		Shaft - Toe	Soil Profile Code	
APILE	CAPWAP	Clay - Clay	1	101
		Clay - Mixed	2	19
		Clay - Sand	3	44
		Mixed - Clay	4	53
		Mixed - Mixed	5	28
		Mixed - Sand	6	109
		Sand - Clay	7	20
		Sand - Mixed	8	11
		Sand - Sand	9	183
APILE	PDA	Clay - Clay	1	106
		Clay - Mixed	2	19
		Clay - Sand	3	44
		Mixed - Clay	4	53
		Mixed - Mixed	5	28
		Mixed - Sand	6	108
		Sand - Clay	7	20
		Sand - Mixed	8	11

		Sand - Sand	9	183

Table 6: Detailed Data Set for Case C

Prediction Method	Measured Method	Data set C			Number of Piles
		Material Type	Shaft - Toe	Soil Profile Code	
APILE	CAPWAP	PSC	Clay - Clay	1	41
			Clay - Mixed	2	5
			Clay - Sand	3	26
			Mixed - Clay	4	25
			Mixed - Mixed	5	17
			Mixed - Sand	6	48
			Sand - Clay	7	8
			Sand - Mixed	8	9
			Sand - Sand	9	60
		HP	Clay - Clay	1	61
			Clay - Mixed	2	14
			Clay - Sand	3	18
			Mixed - Clay	4	24
			Mixed - Mixed	5	9
			Mixed - Sand	6	59
			Sand - Clay	7	11
			Sand - Mixed	8	2
			Sand - Sand	9	111
		SPP	Mixed - Clay	4	4
			Mixed - Mixed	5	2
			Mixed - Sand	6	2
			Sand - Sand	9	12
APILE	PDA	PSC	Clay - Clay	1	41
			Clay - Mixed	2	5
			Clay - Sand	3	26
			Mixed - Clay	4	25
			Mixed - Mixed	5	17
			Mixed - Sand	6	47
			Sand - Clay	7	8
			Sand - Mixed	8	9
			Sand - Sand	9	61
		HP	Clay - Clay	1	65

			Clay - Mixed	2	14
			Clay - Sand	3	18
			Mixed - Clay	4	24
			Mixed - Mixed	5	9
			Mixed - Sand	6	59
			Sand - Clay	7	11
			Sand - Mixed	8	2
			Sand - Sand	9	110
		SPP	Mixed - Clay	4	4
			Mixed - Mixed	5	2
			Mixed - Sand	6	2
			Sand - Sand	9	12

Table 7: Detailed Data Set for Case D

Prediction Method	Measured Method	Soil Regions	Number of Piles
APILE	CAPWAP	Quaternary	191
		Tertiary All	336
		Tertiary, Soil profile codes: 1-4-7	130
		Tertiary, Soil profile codes: 3-6-9	150
		Cretaceous	38

APILE	PDA	Quaternary	192
		Tertiary All	339
		Tertiary Soil profile codes: 1-4-7	134
		Tertiary Soil profile codes: 3-6-9	149
		Cretaceous	38

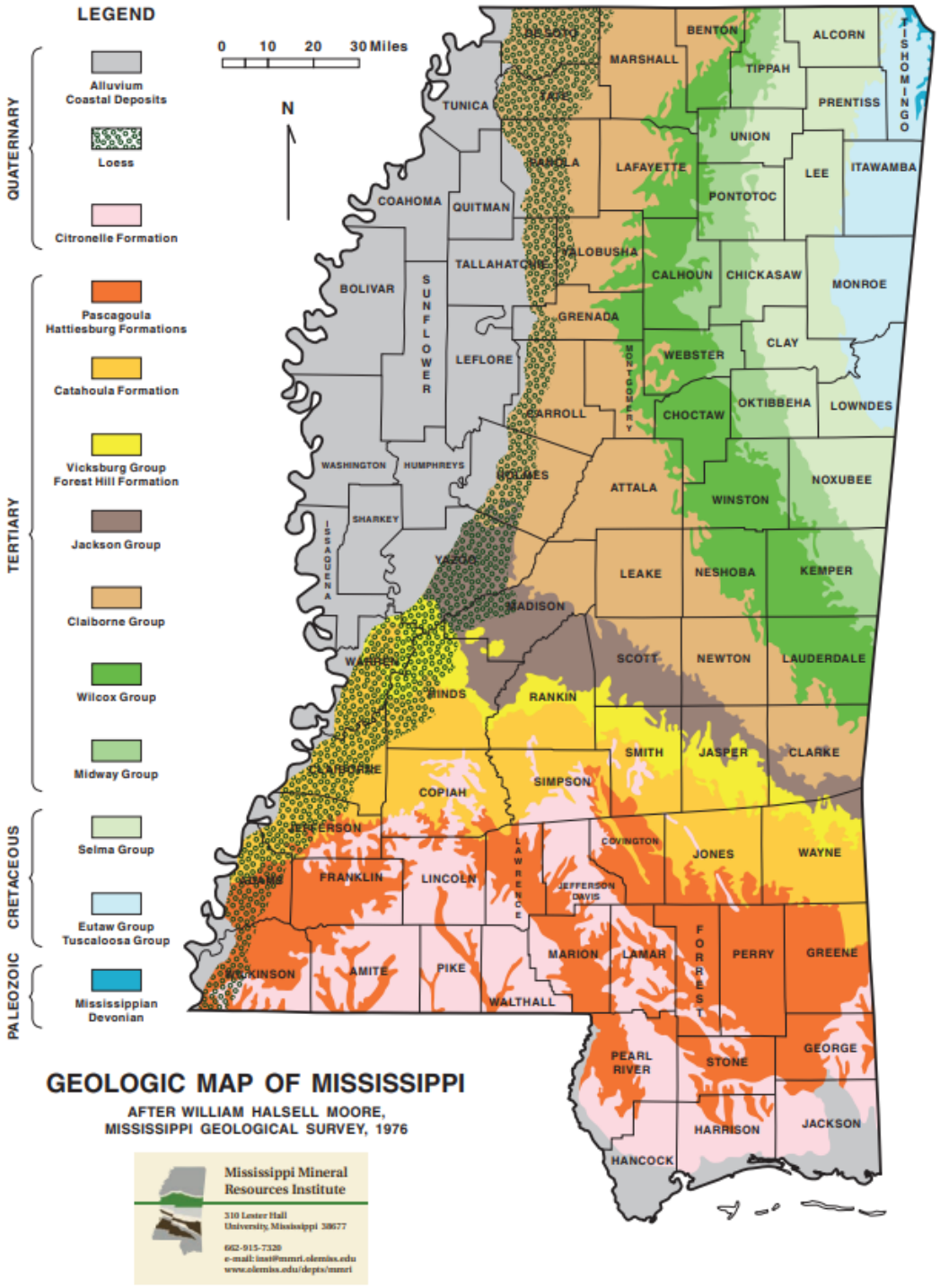

Figure 8: Geologic map of the state of Mississippi (Mississippi Mineral Resources Institute).

3.4 Calibration Methodology

This section describes the concepts and probabilistic-based methodologies applied to a LRFD calibration. These methodologies are based on random variables and the statistical characterization of their bias values. This section also explains how to conduct an actual calibration and apply it to the development of LRFD design specifications. Also, the First Order Second Moment (FOSM) calibration, the First Order Reliability Method (FORM) calibration, and the Monte Carlo Simulation (MCS) calibration concepts and procedures are explained.

3.4.1 Random Variables and Bias

This section defines the concept of random variables and bias, which both compose the basis to perform the LRFD calibration. First of all, Allen et al. [8] define a random variable as a variable that does not have an exact value and it pertains to a set of values, or a range, and the probability of occurrence. Nowak and Collins [29], add that a random variable is a function that maps events onto intervals on the axis of real numbers. A probability function is defined on events and this definition can be extended by random variables. Figure 9 shows a schematic representation of a random variable as a function. For LRFD methodology in driven piles, the random variables consist of loads (dead and live loads) and resistances (capacity).

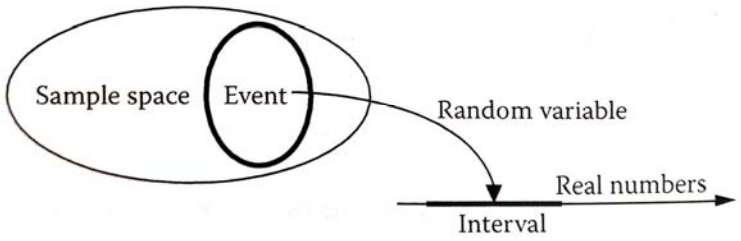

Figure 9: Schematic representation of a random variable as a function (Nowak and Collins, 2013).

Second, the definition of bias is the ratio of the true parameter value and the expected value. Within structural reliability field, the bias is the ratio of the measured (actual) to the nominal (predicted) value. The bias allows the soil characteristics, materials, and construction uncertainties to be included into a design method. Thus, a calibration must be performed for each prediction method independently. In this study, the bias for loads (λ_Q) and resistance (λ_R) are calculate as follows:

$$\lambda_Q = \frac{Q_m}{Q_p} \text{ and} \tag{9}$$

$$\lambda_R = \frac{R_m}{R_p}, \tag{10}$$

where Q_m is the measured load, Q_p is the predicted load, R_m is the measured resistance, and R_p is the predicted resistance.

It is important to mention that a bias must be calculated for every pair (measured and predicted) of data, and then, they shall be grouped to obtain some of their basic descriptive statistical features, which are explained in the next section.

3.4.2 Mean, Standard deviation, and Coefficient of Variation of random variables.

Once the bias values have been calculated for each pile, the mean, standard deviation, and the coefficient of variation shall be calculated for each data case. As mentioned by Allen et al. [8], the mean, standard deviation, and coefficient of variation from the random variables considered in the limit state equation are necessary to perform the resistance factor calibration. In this study, the mean, standard deviation, and coefficient of variation values correspond to the bias random resistance values and bias random load variables since they are present in the limit state equation. Paikowsky et al. [5], states that load and resistance random variables can be taken as normal or lognormal distributed variables and both type of distributions are defined in the following sections. For a normal distribution, the mean ($\widehat{\mu_x}$) is the sum of the individual values from a sample divided by the total number of values *n*.

$$\widehat{\mu_x} = \frac{X_i + X_3 + \cdots + X_i}{n}. \tag{11}$$

The second parameter is the standard deviation (σ_x or $\widehat{\sigma_x}$), which *measures of the dispersion about the mean of the data representing the random variable* [8]. For a population, it can be calculated as follows:

$$\sigma_x = \sqrt{\frac{\sum_{i=1}^{n}(X_i - \mu)^2}{N}}. \quad (12)$$

For a sample (from a larger population), the standard deviation can be calculated as follows:

$$\widehat{\sigma_x} = \sqrt{\frac{\sum_{i=1}^{n}(X_i - \mu)^2}{n-1}}. \quad (13)$$

Lastly, the coefficient of variation (*COV* or V_x) is the third statistical value required for the LRFD calibration. Nonetheless, the COV is not actually considered a third statistical parameter because it is just the standard deviation normalized by the mean. Therefore, other calibration documents just state the mean and COV or the mean and the standard deviation as initial calibration values. The COV is unitless and can be calculated as follows:

$$COV_x = V_x = \frac{\widehat{\sigma_x}}{\widehat{\mu_x}}. \quad (14)$$

Sometimes the term *variance* is used, however, both terms are different. The actual variance is a unit dependent value equals to the square of the standard deviation and it is not specifically used in this study for calibration purposes.

3.4.3 FOSM calibration concept and procedure.

The First Order Second Moment (FOSM) is a closed form solution and a probabilistic reliability method [30]. It is called FOSM because it is a first-order expansion about the mean value and a linear approximation of the second corrected moment (variance) [31]. This method was developed largely by Cornell [32] and Lind [33]. FOSM belongs to the level II of probabilistic-based analysis. FOSM is one of the two methods used by AASHTO specifications [14] for calibrating LRFD resistance factors. This method involves the consideration of statistical characteristics such as the mean, standard deviation, and coefficient of variation (COV) to describe the probability functions of the load and resistance variables. FOSM assumes that the

load and resistance random variables are modeled following a lognormal distribution [6]. The procedure is listed below:

Step 1: Obtain the bias mean, standard deviation, and COV of the load and resistance values independently using equations 21 to 24. Moreover, the load factors for the dead load and live loads shall be known.

Step 2: Establish the target reliability index based on the probability of failure desired.

Step 3: According to Cornell [32] and Lind [33], the following equation can be used to compute the resistance factor:

$$\phi_R = \frac{\lambda_R\left(\frac{\gamma_{QD}Q_D}{Q_L} + \gamma_{QL}\right)\sqrt{\left[\frac{1 + COV_{QD}^2 + COV_{QL}^2}{1 + COV_R^2}\right]}}{\left(\frac{\lambda_{QD}Q_D}{Q_L} + \lambda_{QL}\right)\exp\{\beta_T\sqrt{\ln[(1 + COV_R^2)(1 + COV_{QD}^2 + COV_{QL}^2)]}\}}, \quad (15)$$

where ϕ_R is the calibrated resistance factor, λ_R is the mean resistance bias factor, λ_{QD} is the dead load bias factor, λ_{QL} is the live load bias factor, β_T is the target reliability index, COV_{QD} is the coefficient of variation for dead load, COV_{QL} is the coefficient of variation for live load, and COV_R is the coefficient of variation for resistance.

3.4.4 FORM Calibration concept and procedure.

FORM means First Order Reliability Method (FORM) because it is based in the first-order terms in the Taylor series expansion, where only means and variances are required [29]. NCHRP 507 [5] states that the structural design codes used FORM calibration, hence Geotechnical resistance factors shall follow the same methodology in order to be consistent when using the load factors. In addition, the same report [5] mentions that FORM resistance factors are about 10% higher than FOSM resistance factors. The procedure listed in this report follows the actual FORM procedure (not Hasofer-Lind method), which is based on Styler thesis [6]; and Phoon, Kulhawy, and Grigoriu's paper [34].

Step 1: Define the failure equation

The failure equation is adapted from the limit state equation and consists on the relation used to represent a specific limit state of a system of variables. Failure takes place when

the failure equation is less than or equal to zero. The failure equation is usually the difference between the resistance and the load random variables:

$$G = R - Q, \quad (16)$$

where R is the resistance random variable and Q is the load random variable. Thus, When G is less than or equal to zero, failure of the system occurs. It should be noted that no loading factors are used in this equation. These R and Q random variables are function of the bias factor variables:

$$R = r_n * \lambda_R \text{ and} \quad (17)$$

$$Q = \left(q_D * \lambda_{QD}\right) + (q_L \lambda_{QL}), \quad (18)$$

where r_n is the nominal (predicted) resistance, q_D is the dead load value, and q_L is the live load value.

Step 2: Choose random variable distributions

The distributions of the random variables will typically be considered as normal or lognormal. The case of calibration of driven piles, Paikowsky et al. [5] suggests taking bias factors as lognormal random variables. However, Styler [6] suggest performing a chi-squared test to justify a chosen random variable.

Step 3: Choose LRFD factors to analyze

The probability of failure is based on the load factors, the specific reliability index, and the dead to live load ratio. Usually, load factors are specified by organization. The case of driven pile reliability indices and dead to live ratios, the values are discussed and stated by Paikowsky et al. [5]. When using the FORM calibration, a resistance factor is computed for its corresponding reliability index. Therefore, multiple resistance factors will be required to be computed to match the target reliability index.

Styler [6] contends that the design space is separated from the failure space due to the load and resistance factors. A design point is based on the LRFD limit equation; however, the randomness of the bias factors results in unknown exact resistance and load values. FORM method determines the probability that the actual resistance and load occurs within the failure space for a specific design that takes place on the boundary of the

acceptable design space. The slope of the design space can be computed from the dead to live load ratio and the load and resistance factors as follows:

$$\phi_R * r_n = (\gamma_{QD} * q_D) + (\gamma_{QL} * q_L)\,, \tag{19}$$

$$q_D/q_L = \eta\,, \tag{20}$$

$$\phi_R * r_n = (\gamma_{QD} * \eta * q_L) + (\gamma_{QL} * q_L), \tag{21}$$

$$\phi_R * r_n = q_L(\eta * \gamma_{QD} * \gamma_{QL}), \tag{22}$$

$$q_L = \frac{\phi_R * r_n}{\eta * \gamma_{QD} + \gamma_{QD}}\,, \tag{23}$$

$$q_D = \eta * q_L = \frac{\eta * \phi_R * r_n}{\eta * \gamma_{QD} + \gamma_{QD}}\,, \text{and} \tag{24}$$

$$Slope = \frac{q}{r} = \frac{q_D + q_L}{r_n} = \frac{\frac{\eta * \phi_R * r_n}{\eta * \gamma_{QD} * \gamma_{QL}} + \frac{\phi_R * r_n}{\eta * \gamma_{QD} + \gamma_{QL}}}{r_n} = \frac{\phi_R}{\eta * \gamma_{QD} + \gamma_{QL}}(\eta + 1), \tag{25}$$

where γ_{QD} is the dead load factor, γ_{QL} is the live load factor, η is the dead-to-live load ratio.

Step 4: Calculate the initial design point

The FORM calibration starts at this step. Using the given nominal resistance and dead to live load ratio, the dead and live loads can be computed as follows:

$$\phi_R * r_n = (\gamma_{QD} * q_D) + (\gamma_{QL} * q_L)\,, \tag{26}$$

$$\frac{q_D}{q_L} = \eta\,, \tag{27}$$

$$q_D = \eta * q_L\,, \tag{28}$$

$$\phi_R * r_n = q_L(\gamma_{QD}\eta + \gamma_{QL})\,, \text{and} \tag{29}$$

$$q_L = \frac{\phi_R * r_n}{\gamma_{QD} * \eta + \gamma_{QL}}, \tag{30}$$

As mentioned before, the resistance and load random variables are function of the lognormal bias random variables.

$$R = r_n * \lambda_R \text{ and} \tag{31}$$

$$Q = q_D * \lambda_{QD} + q_L * \lambda_{QL} . \tag{32}$$

Likewise, the expected values for the *R* and *Q* random variables are calculated using the following equations:

$$E[R] = r_n * \lambda_R \text{ and} \tag{33}$$

$$E[Q] = (q_D * \lambda_{QD}) + (q_L * \lambda_{QL}) \tag{34}$$

where $E[R]$ is the expected value of the resistance random variable, and $E[Q]$ is the expected value of the load random variable. Then, the normal standard deviation for the resistance and load can be computed as follows:

$$\sigma_R = r_n \sigma_{\lambda R} \text{ and} \tag{35}$$

$$\sigma_Q = \sqrt{q_D^2 \sigma_{\lambda D}^2 + q_L^2 \sigma_{\lambda L}^2} \tag{36}$$

where σ_R is the standard deviation of the resistance R, σ_Q is the standard deviation of the load Q, $\sigma_{\lambda R}$ is the standard deviation of the resistance dataset, $\sigma_{\lambda D}$ the standard deviation of the dead load dataset, and $\sigma_{\lambda Q}$ the standard deviation of the live load dataset.

Step 5: Transform into an equivalent normal distribution

In this step, it is necessary to transform an equivalent normal distribution using the design point (*r, q*). For the first iteration, the design point is equal to the expected resistance and load random values (*E[R], E[Q]*). The mean and standard deviation can be computed with the following equations:

$$\sigma_{RN} = \frac{\phi(\Phi^{-1}(F_R(r)))}{f_R(r)}, \tag{37}$$

$$[R_N] = r - \Phi^{-1}(F_R(r))\sigma_{RN} , \tag{38}$$

$$\sigma_{QN} = \frac{\phi\left((\Phi^{-1}\left(F_Q(q)\right)\right)}{f_q(q)} \text{ , and} \tag{39}$$

$$[Q_N] = q - \Phi^{-1}(F_Q(q))\sigma_{QN} , \tag{40}$$

Where $E[R_N]$ is the expected equivalent normal random variable for the resistance, and $E[Q_N]$ is the expected equivalent normal random variable for the load. The function Φ^{-1} represents the inverse of the standard cumulative distribution function. $F_R(r)$ represents the cumulative function for random variable R. It should be noted that the pdf depends of the chosen distribution.

Styler [6] says that when FORM is performed, the lognormal random variable is positively biased, and the mean of the resulting normal random is lower.

Step 6: Transform original random variables to standard normal random variables

To perform this transformation, the following equations are required:

$$R_{SN} = \frac{R - E[R_N]}{\sigma_{RN}} \text{ and} \tag{41}$$

$$Q_{SN} = \frac{Q - E[Q_N]}{\sigma_{QN}}, \tag{42}$$

where R and Q are the original lognormal random variables, and R_{SN} and Q_{SN} are the standard normal random variables for resistance and load, respectively. In the same way, the design point shall be transformed from real space to standard normal random variable space. It should be noted that in the first iteration, the design point in real space is the most probable values of the resistance and load lognormal random variables. In other words, the design point is the mode of the lognormal distribution. Thus, the standard normal space design point shall be calculated from the real space design point using the following equations:

$$r = \frac{E[R] - E[R_N]}{\sigma_{RN}} \text{ and} \tag{43}$$

$$q = \frac{E[Q] - E[Q_N]}{\sigma_{QN}}. \tag{44}$$

Step 7: Rewrite the failure in terms of the standard normal random variables

It is important to transform the failure equation to standard normal random variables using the following equations:

$$G = R - Q \text{ and} \tag{45}$$

$$G' = (R_{SN}\sigma_{RN} + E[R_N]) - (Q_{SN}\sigma_{QN} + E[Q_N]). \tag{46}$$

Step 8: Compute a new trial design point

Styler [6] states that a new trial design point (r^*, q^*) shall be computed using the following equations:

$$r^* = \frac{(-E[R_N] + E[Q_N])\sigma_{RN}}{(\sigma_{RN})^2 + (\sigma_{QN})^2} \text{ and} \quad (47)$$

$$q^* = \frac{(-E[R_N] + E[Q_N])\sigma_{QN}}{(\sigma_{RN})^2 + (\sigma_{QN})^2}. \quad (48)$$

This new design point represents the closest distance from the origin to this failure line. It should be noted that the failure line barely varies after each iteration.

Step 9: Calculate the reliability index.

The reliability index is the closest distance from the origin to the failure line and can be calculated as follow:

$$\beta = \sqrt{(r^*)^2 + (q^*)^2}. \quad (49)$$

Step 10: Repetitive iteration (FORM iteration)

The new design point shall be transformed back to the real space using the following equations:

$$r = r^*\sigma_{RN} + E[R_N], \text{and} \quad (50)$$

$$q = q^*\sigma_{QN} + E[Q_N] \quad (51)$$

Then, recalculate the equivalent normal distribution using this new design point (r, q). This procedure must be repeated until the reliability index β remains stable as shown in the Figure 10.

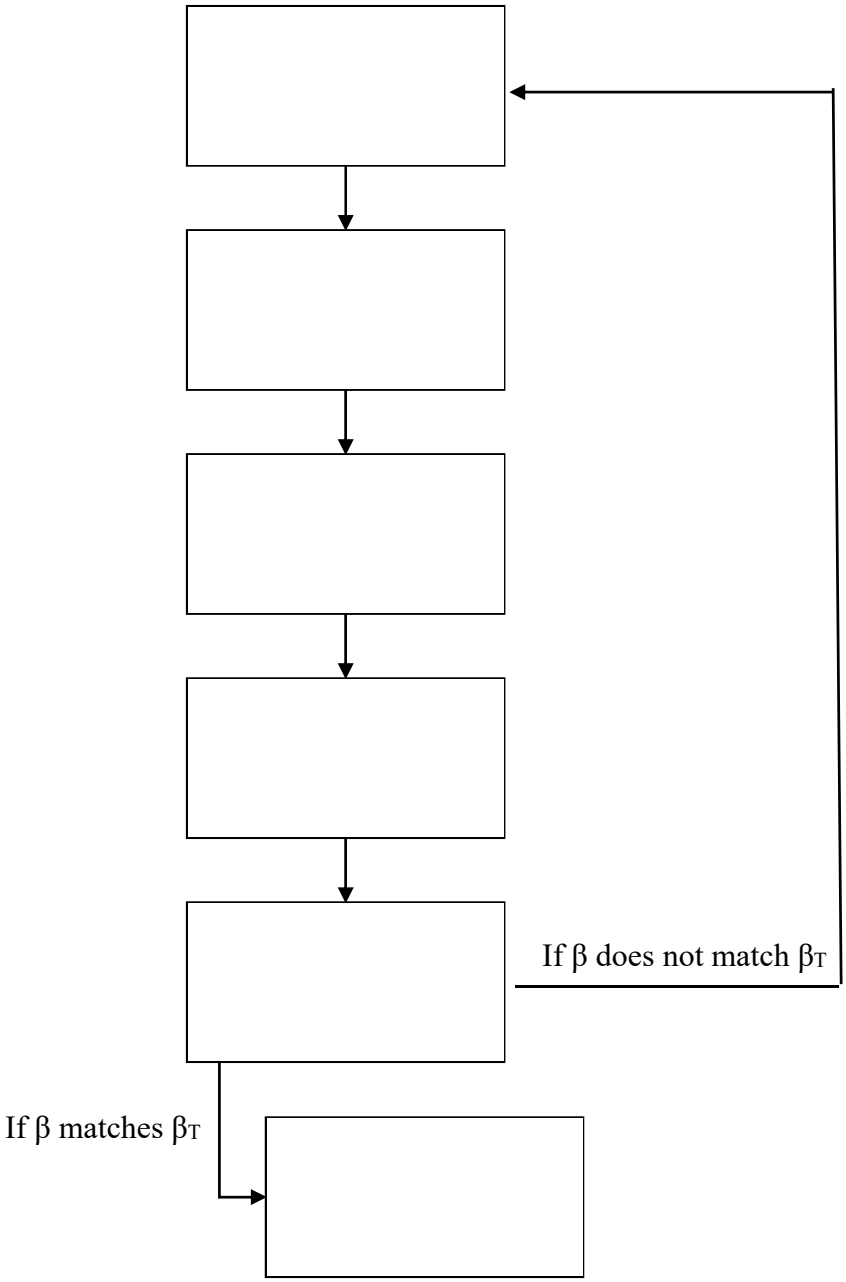

Figure 10: Iteration procedure flowchart from Step 9.

Finally, the resistance factor established in the step 3 shall be altered until the reliability index β matches the target reliability index β_T. The resistance factor that satisfies the target reliability index is the final FORM calibrated resistance factor.

3.4.5 Monte Carlo simulation concept and procedure

Nowak and Collins [29] mention that the basic idea of the Monte Carlo Simulation (MCS) is based on numerically simulating some phenomenon and then observing the number of times some event of interest occurs. Moreover, Allen et al. [8] states that Monte Carlo Simulation is simply a tool to curve fit and extrapolate available measured statistical data; in this case, load and resistance data, or more generally, for any random variable that affects the outcome of a limit state calculation. According to Nowak and Collins [29], the Monte Carlo Simulation is generally applied to the following cases:

- It is used when closed-form solutions are not possible or extremely difficult.
- It is used when closed-form solutions require too many simplifying assumptions.
- It is used to revise the results provided from other solution techniques.

The Monte Carlo procedure stated in this report is extracted from Allen et al. [8] and Reddy and Stuedlein [35] in order to present a detailed and understandable procedure. MCS calibration is performed to revise the resistance and efficiency factors from FOSM and FORM in this study. The procedure is listed below.

Step 1: It is first important to establish a limit state function. According to AASHTO [36], for geotechnical and structural design, the basic limit state function is expressed as:

$$\phi_R R_n \geq \sum_{j=1}^{k} \gamma_Q Q_n \,. \tag{52}$$

This equation represents failure when the applied loads are equal to the available resistance. However, Reddy and Stuedlein [35] contend that for calibration purposes, the limit state equation shall be expressed in terms of distribution in the margin of safety (g_i), and the load and resistance biases as [37]:

$$g_i = \lambda_{R,i} \frac{\gamma_{avg}}{\varphi_R} - \lambda_{Q,i} \geq 0 \,, \tag{53}$$

where γ_{avg} is a weighted load factor representing multiple load sources and λ_Q is the bias of the applied load. Stuedlein et al. [38] says that in case of multiple load sources (such as bridges and other superstructures), λ_Q can be computed as follows:

$$\lambda_{Q,i} = \lambda_Q = \frac{\lambda_{QD}\eta + \lambda_{QL}}{\eta + 1}, \tag{54}$$

where λ_{QD} is the bias for dead loads, λ_{QL} is the bias for live loads, and η is the ratio of the dead to live load. Stuedlein et al. [38] adds that in cases of having multiple loads, a weighted load factor may be used:

$$\Upsilon_{avg} = \frac{\lambda_{QD}\gamma_{QD}\eta + \lambda_{QL}\gamma_{QL}}{\lambda_{QD}\eta + \lambda_{QL}}, \tag{55}$$

where $\gamma_{Q,D}$ is the dead load factor, and $\gamma_{Q,L}$ is the live load factor.

Step 2: Establish the reliability-target value β_T, which is a function of the probability of failure p_f. Paikowsky et al. [5] indicates that redundant piles (groups of 5 piles or more) require a β_T of 2.33. On other hand, non-redundant piles require a β_T of 3.0.

Step 3: Establish the number of simulations (*N)* required prior to performing the simulation. This can be calculated according to the true probability of failure $P_{f\ true}$ established, which corresponds to the target reliability index, and the coefficient of variation of the estimate probability V_p as follows:

$$N = \frac{1 - P_{f\ true}}{\left(V_p^2\right) * P_{f\ true}}. \tag{56}$$

Step 4: The data is extrapolated (simulation) following the distributions of the two variables *Q* and *R*. This simulation is performed considering three statistical parameters that characterize the data: mean, standard deviation, and cumulative distribution function (cdf). It should be noted that the closed-form methods use just the mean and the standard deviation. In case of load and resistance values, they may be considered as normal or lognormal random variables.

In case *Q* has a normal distribution, randomly determined data shall be generated in accordance to the specified distribution characterized by a mean, a standard deviation, and a coefficient of variation using a random number generator as shown below [29]:

$$Q_i = \lambda_Q(1 + COV_Q z_{i-Q}), \tag{57}$$

where Q_i is a randomly generated value of Q using a specified set of statistical parameters, z_i is the inverse normal function of u_{ia} and is equal to $\Phi^{-1}(u_{ia})$, u_{ia} is a random number between 0 and 1 representing a probability of occurrence.

In case Q has a lognormal distribution, randomly determined data shall be generated in accordance to the specified distribution characterized by lognormal mean, a lognormal standard deviation, and a coefficient of variation using a random number generator as shown below [29]:

$$Q_i = exp(\mu_{ln-Q} + \sigma_{ln-Q} z_{i-Q}) \text{ and} \tag{58}$$

where:

$$\mu_{ln-Q} = LN(\lambda_Q) - 0.5\sigma_{ln-Q}^2 \text{ , and} \tag{59}$$

$$\sigma_{ln-Q} = \{LN[(COV_Q)^2 + 1]\}^{0.5} . \tag{60}$$

Similarly, the resistance values R have a lognormal distribution. Thus, randomly determined data shall be generated in accordance to the specified distribution characterized by a mean, a standard deviation, and a coefficient of variation using a random number generator as shown below:

$$R_i = \exp(\mu_{ln-R} + \sigma_{ln-R} z_{i-R}) , \tag{61}$$

where:

$$\mu_{ln-R} = LN(\lambda_R) - 0.5\sigma_{ln-R}^2 , \tag{62}$$

$$\sigma_{ln-R} = \{LN[(COV_R)^2 + 1]\}^{0.5}, \tag{63}$$

and where R_i is a randomly generated value of R using a specified set of statistical parameters, z_i is the inverse normal function of u_{ib} and is equal to $\Phi^{-1}(u_{ib})$, u_{ib} is a random number between 0 and 1 representing a probability of occurrence.

It is important to mention that the random numbers u_{ia} and u_{ib} shall be generated independently assuming that Q and R are independent variables [8].

Step 5: Once the simulated data for each distribution has been generated, set a trial resistance factor and the limit state function g is computed for each couple of Q and R values.

Step 6: Determine the probability of failure of the simulation performed using the following equation:

$$P_f = \frac{n}{N}, \tag{64}$$

where *n* is the number of times that a particular criterion is achieved. In this case *n* is the number of times when *g* is lower than zero (which indicates failure). *N* is the number of simulations performed.

Step 7: Calculate the reliability index using the probability of failure computed in the previous step. It can be calculated in Microsoft Excel using the function NORMSINV as shown:

$$\beta = NORMSINV(P_f). \tag{65}$$

Step 8: Set different values for the resistance factor until β and β_T converge. The final resistance factor has been calculated.

3.5 Reliability Based Efficiency Factor

The values of the calibrated resistance factor alone do not represent an objective measurement of the design method efficiency. Such efficiency can be better measured if the efficiency factor is considered [39], which can be calculated as follows:

$$Efficiency\ factor = \frac{\phi_R}{\lambda_R}, \tag{66}$$

where ϕ_R is the calibrated resistance factor by each method, and λ_R is the mean bias resistance. According to NCHRP 507 [5] and Figure 11, the efficiency factor is systematically higher for methods which predict more accurately regardless of the bias. In this way, a design or prediction method can be more efficient only if its variability (COV) is reduced. The ideal method would have a bias factor of 1, a COV of 0, hence a resistance factor of 0.80. It is suggested to choose the design methods according to their COV [5].

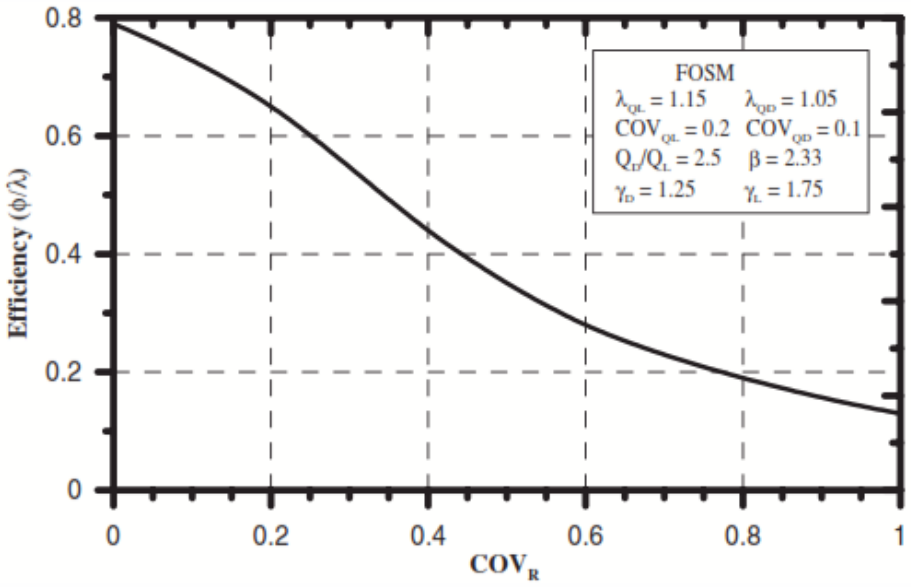

Figure 11: Illustration of the efficiency factor as a measure of the effectiveness of a design method when using resistance factors (Paikowsly et al, 2004)

Jabo [40] adds that computing a higher resistance factor does not necessarily imply an efficient pile design method. While reducing the standard deviation (σ) value would always improve the precision of the prediction method, increasing the λ_R could make prediction overestimate the pile capacity. Therefore, the economy factor of the structure would be affected. In addition, Jabo [40] states that the design equation for an axial pile can be rewritten as follows:

$$P_{design} = \phi_R R_n, \tag{67}$$

where P_{design} is the design pile capacity, ϕ_R is the calibrated resistance factor, and R_n is the nominal resistance of the pile. If the resistance bias factor λ_R is defined as the ratio of measured resistance (R_m) to predicted nominal resistance (R_n), the equation 66 can be modified as follows:

$$P_{design} = \left(\frac{\phi_R}{\lambda_R}\right) R_m. \tag{68}$$

Using this relationship, Jabo [40] demonstrates that *only a portion of the measured capacity is allowed for design to meet the required reliability level*. Consequently, the efficiency

factor can efficiently quantify the performance of the pile design method. To put it briefly, a higher efficiency factor implies a better pile design method [39].

3.6 LFRD Resistance Factors Calibration

3.6.1 Target Reliability Index

The target reliability index represents the probability of failure desired. Therefore, it determines magnitude of the load and resistance factors for a LRFD calibration. In this project, the reliability index and probability of failure are obtained from the Federal Highway Administration [13], Paikowsky et al. [5], and Luna [3] as shown in Table 8.

Table 8: Reliability index values based on pile groups

Pile Group type	β	P*f*
Redundant (5 or more piles per pile cap)	2.33	1.00%
Intermediate point between redundant and non-redundant piles	2.50	0.99%
Non-redundant (4 or fewer piles per pile cap)	3.00	0.10 %

3.6.2 Dead and Live loads characterization

Prior to performing the calibration of resistance factors, the statistical characteristics of the dead and lives loads shall be known as well as the load factors. In this report, the values used by AASHTO [14] and suggested by Paikowsky [5] are used. These values are shown in the Table 9.

Table 9: Load statistical values used.

Dead Load		Live Load	
Parameter	**Recommended value**	**Parameter**	**Recommended value**
λ_{QD}	1.050	λ_{QL}	1.150
COV_{QD}	0.100	COV_{QL}	0.200
$\sigma_{\lambda D}$	0.105	$\sigma_{\lambda L}$	1.230

γ_{QD}	1.250	γ_{QL}	1.750

In addition, Paikowsky et al. [5] indicates that a dead-to-live ratio of 2 or 2.5 is reasonable due to the small influence of this factor on the calibrated resistance factors. Therefore, in this report, the value for Q_D/Q_L is taken as 2 and can be also represented by the symbol η.

CHAPTER IV - RESEARCH FINDINGS

This chapter presents the preliminary results of the LRFD calibration of resistance factors. The results for each prediction or construction control method, each calibration method, each data sets, data cases, and target reliability index, are organized in tables and graphs for a better understanding. Estimated setup factors results are also presented in this chapter.

4.1 Preliminary Resistance Factors

Tables 10 to 13 present the preliminary resistance factors obtained through FOSM, FORM, and Monte Carlo Simulation, for CAPWAP and PDA, as well as an average between the three methods, for all data sets, data cases, and target reliability index. The tables include the summary of the statistics of the mean resistance bias, along with the individual resistance factors φ_R and efficiency factors for every calibration method.

Table 10: Preliminary resistance factors for Data Case A

Design Method	Material Type	# of Piles	Mean (λ_R)	COV_R	β	FOSM		FORM		MC		Average	
						φ_R	φ_R/λ	φ_R	φ_R/λ	φ_R	φ_R/λ	φ_R	φ_R/λ
CAPWAP	All Piles	648	1.499	0.726	3.00	**0.21**	0.14	**0.22**	0.15	**0.23**	0.15	**0.22**	0.15
					2.50	**0.30**	0.20	**0.31**	0.21	**0.32**	0.21	**0.31**	0.21
					2.33	**0.33**	0.22	**0.35**	0.23	**0.35**	0.23	**0.34**	0.23
	PSC	279	1.651	0.633	3.00	**0.29**	0.18	**0.31**	0.19	**0.32**	0.19	**0.31**	0.19
					2.50	**0.40**	0.24	**0.42**	0.25	**0.44**	0.27	**0.42**	0.25
					2.33	**0.45**	0.27	**0.47**	0.28	**0.49**	0.30	**0.47**	0.28
	HP	347	1.437	0.782	3.00	**0.17**	0.12	**0.18**	0.13	**0.19**	0.13	**0.18**	0.13
					2.50	**0.25**	0.17	**0.26**	0.18	**0.27**	0.19	**0.26**	0.18
					2.33	**0.28**	0.20	**0.29**	0.20	**0.29**	0.20	**0.29**	0.20
	SPP	22	0.564	0.368	3.00	**0.20**	0.36	**0.23**	0.41	**0.24**	0.43	**0.22**	0.40
					2.50	**0.25**	0.45	**0.27**	0.48	**0.28**	0.50	**0.27**	0.47
					2.33	**0.27**	0.48	**0.29**	0.51	**0.30**	0.53	**0.29**	0.51
PDA	All Piles	652	1.583	0.677	3.00	**0.25**	0.16	**0.26**	0.16	**0.27**	0.17	**0.26**	0.16
					2.50	**0.35**	0.22	**0.36**	0.23	**0.37**	0.23	**0.36**	0.23
					2.33	**0.39**	0.25	**0.41**	0.26	**0.40**	0.25	**0.40**	0.25
	PSC	280	1.675	0.603	3.00	**0.32**	0.19	**0.34**	0.20	**0.35**	0.21	**0.34**	0.20
					2.50	**0.44**	0.26	**0.46**	0.27	**0.46**	0.27	**0.45**	0.27
					2.33	**0.48**	0.29	**0.51**	0.30	**0.52**	0.31	**0.50**	0.30
	HP	350	1.563	0.722	3.00	**0.22**	0.14	**0.23**	0.15	**0.23**	0.15	**0.23**	0.15
					2.50	**0.31**	0.20	**0.32**	0.20	**0.33**	0.21	**0.32**	0.20
					2.33	**0.22**	0.14	**0.36**	0.23	**0.37**	0.24	**0.32**	0.20
	SPP	22	0.734	0.337	3.00	**0.29**	0.39	**0.33**	0.45	**0.33**	0.45	**0.32**	0.43
					2.50	**0.35**	0.48	**0.39**	0.53	**0.39**	0.53	**0.38**	0.51

					2.33	**0.38**	0.51	**0.41**	0.56	**0.42**	0.57	**0.40**	0.55

Table 11: Preliminary resistance factors for Data Case B

Design Method	Soil Profile Code	# of Piles	Mean (λ_R)	COV_R	β	FOSM		FORM		MC		Average	
						φ_R	φ_R/λ	φ_R	φ_R/λ	φ_R	φ_R/λ	φ_R	φ_R/λ
CAPWAP	1	101	1.563	0.577	3.00	**0.32**	0.20	**0.35**	0.22	**0.35**	0.22	**0.34**	0.22
					2.50	**0.43**	0.28	**0.46**	0.29	**0.46**	0.29	**0.45**	0.29
					2.33	**0.47**	0.30	**0.5**	0.32	**0.5**	0.32	**0.49**	0.31
	2	19	1.398	0.494	3.00	**0.36**	0.26	**0.39**	0.28	**0.39**	0.28	**0.38**	0.27
					2.50	**0.46**	0.33	**0.5**	0.36	**0.5**	0.36	**0.49**	0.35
					2.33	**0.5**	0.36	**0.54**	0.39	**0.54**	0.39	**0.53**	0.38
	3	44	1.898	0.807	3.00	**0.21**	0.11	**0.23**	0.12	**0.23**	0.12	**0.22**	0.12
					2.50	**0.31**	0.16	**0.33**	0.17	**0.32**	0.17	**0.32**	0.17
					2.33	**0.35**	0.18	**0.37**	0.19	**0.38**	0.20	**0.37**	0.19
	4	53	1.319	0.614	3.00	**0.24**	0.18	**0.27**	0.20	**0.27**	0.20	**0.26**	0.20
					2.50	**0.33**	0.25	**0.35**	0.27	**0.35**	0.27	**0.34**	0.26
					2.33	**0.37**	0.28	**0.39**	0.30	**0.39**	0.30	**0.38**	0.29
	5	28	1.399	0.497	3.00	**0.35**	0.25	**0.39**	0.28	**0.4**	0.29	**0.38**	0.27
					2.50	**0.46**	0.33	**0.5**	0.36	**0.49**	0.35	**0.48**	0.35
					2.33	**0.5**	0.36	**0.54**	0.39	**0.55**	0.39	**0.53**	0.38
	6	109	1.422	0.610	3.00	**0.27**	0.19	**0.29**	0.20	**0.3**	0.21	**0.29**	0.20
					2.50	**0.36**	0.25	**0.39**	0.27	**0.39**	0.27	**0.38**	0.27
					2.33	**0.4**	0.28	**0.43**	0.30	**0.42**	0.30	**0.42**	0.29
	7	20	1.357	0.352	3.00	**0.51**	0.38	**0.59**	0.43	**0.56**	0.41	**0.55**	0.41
					2.50	**0.62**	0.46	**0.7**	0.52	**0.7**	0.52	**0.67**	0.50
					2.33	**0.66**	0.49	**0.75**	0.55	**0.75**	0.55	**0.72**	0.53
	8	11	1.462	0.458	3.00	**0.41**	0.28	**0.46**	0.31	**0.45**	0.31	**0.44**	0.30
					2.50	**0.52**	0.36	**0.57**	0.39	**0.56**	0.38	**0.55**	0.38
					2.33	**0.57**	0.39	**0.62**	0.42	**0.62**	0.42	**0.60**	0.41
	9	183	1.296	0.747	3.00	**0.17**	0.13	**0.18**	0.14	**0.18**	0.14	**0.18**	0.14
					2.50	**0.24**	0.19	**0.25**	0.19	**0.24**	0.19	**0.24**	0.19
					2.33	**0.27**	0.21	**0.29**	0.22	**0.29**	0.22	**0.28**	0.22
PDA	1	106	1.627	0.534	3.00	**0.37**	0.23	**0.39**	0.24	**0.4**	0.25	**0.39**	0.24
					2.50	**0.49**	0.30	**0.51**	0.31	**0.52**	0.32	**0.51**	0.31
					2.33	**0.54**	0.33	**0.56**	0.34	**0.58**	0.36	**0.56**	0.34
	2	19	1.555	0.450	3.00	**0.45**	0.29	**0.5**	0.32	**0.51**	0.33	**0.49**	0.31
					2.50	**0.57**	0.37	**0.62**	0.40	**0.65**	0.42	**0.61**	0.39
					2.33	**0.62**	0.40	**0.67**	0.43	**0.67**	0.43	**0.65**	0.42
	3	44	1.99	0.776	3.00	**0.24**	0.12	**0.26**	0.13	**0.25**	0.13	**0.25**	0.13
					2.50	**0.35**	0.18	**0.37**	0.19	**0.37**	0.19	**0.36**	0.18
					2.33	**0.39**	0.20	**0.41**	0.21	**0.41**	0.21	**0.40**	0.20
	4	53	1.417	0.564	3.00	**0.3**	0.21	**0.33**	0.23	**0.32**	0.23	**0.32**	0.22
					2.50	**0.4**	0.28	**0.43**	0.30	**0.42**	0.30	**0.42**	0.29
					2.33	**0.44**	0.31	**0.47**	0.33	**0.47**	0.33	**0.46**	0.32
	5	28	1.487	0.496	3.00	**0.38**	0.26	**0.42**	0.28	**0.42**	0.28	**0.41**	0.27
					2.50	**0.49**	0.33	**0.53**	0.36	**0.53**	0.36	**0.52**	0.35
					2.33	**0.53**	0.36	**0.58**	0.39	**0.57**	0.38	**0.56**	0.38
	6	108	1.475	0.506	3.00	**0.36**	0.24	**0.4**	0.27	**0.4**	0.27	**0.39**	0.26
					2.50	**0.47**	0.32	**0.51**	0.35	**0.5**	0.34	**0.49**	0.33
					2.33	**0.52**	0.35	**0.56**	0.38	**0.56**	0.38	**0.55**	0.37

	7	20	1.427	0.373	3.00	**0.5**	0.35	**0.58**	0.41	**0.57**	0.40	**0.55**	0.39
					2.50	**0.62**	0.43	**0.69**	0.48	**0.7**	0.49	**0.67**	0.47
					2.33	**0.67**	0.47	**0.74**	0.52	**0.73**	0.51	**0.71**	0.50
	8	11	1.494	0.398	3.00	**0.49**	0.33	**0.56**	0.37	**0.55**	0.37	**0.53**	0.36
					2.50	**0.62**	0.41	**0.68**	0.46	**0.69**	0.46	**0.66**	0.44
					2.33	**0.66**	0.44	**0.73**	0.49	**0.73**	0.49	**0.71**	0.47
	9	183	1.404	0.685	3.00	**0.22**	0.16	**0.23**	0.16	**0.23**	0.16	**0.23**	0.16
					2.50	**0.3**	0.21	**0.32**	0.23	**0.32**	0.23	**0.31**	0.22
					2.33	**0.33**	0.24	**0.36**	0.26	**0.37**	0.26	**0.35**	0.25

Table 12: Preliminary resistance factors for Data Case C

Design Method	Material Type	Soil Profile Code	# of Piles	Mean (λ_R)	COV_R	β	FOSM		FORM		MC		Average	
							φ_R	φ_R/λ	φ_R	φ_R/λ	φ_R	φ_R/λ	φ_R	φ_R/λ
CAPWAP	PSC	1	41	1.349	0.484	3.00	**0.35**	0.26	**0.39**	0.29	**0.38**	0.28	**0.37**	0.28
						2.50	**0.46**	0.34	**0.49**	0.36	**0.49**	0.36	**0.48**	0.36
						2.33	**0.5**	0.37	**0.54**	0.40	**0.54**	0.40	**0.53**	0.39
		2	5	1.221	0.280	3.00	**0.55**	0.45	**0.64**	0.52	**0.65**	0.53	**0.61**	0.50
						2.50	**0.65**	0.53	**0.75**	0.61	**0.76**	0.62	**0.72**	0.59
						2.33	**0.69**	0.57	**0.79**	0.65	**0.78**	0.64	**0.75**	0.62
		3	26	1.66	0.599	3.00	**0.32**	0.19	**0.35**	0.21	**0.34**	0.20	**0.34**	0.20
						2.50	**0.43**	0.26	**0.46**	0.28	**0.45**	0.27	**0.45**	0.27
						2.33	**0.48**	0.29	**0.51**	0.31	**0.52**	0.31	**0.50**	0.30
		4	25	1.548	0.661	3.00	**0.25**	0.16	**0.27**	0.17	**0.27**	0.17	**0.26**	0.17
						2.50	**0.35**	0.23	**0.37**	0.24	**0.36**	0.23	**0.36**	0.23
						2.33	**0.39**	0.25	**0.41**	0.26	**0.41**	0.26	**0.40**	0.26
		5	17	1.269	0.385	3.00	**0.43**	0.34	**0.49**	0.39	**0.49**	0.39	**0.47**	0.37
						2.50	**0.54**	0.43	**0.6**	0.47	**0.61**	0.48	**0.58**	0.46
						2.33	**0.58**	0.46	**0.64**	0.50	**0.64**	0.50	**0.62**	0.49
		6	48	1.739	0.646	3.00	**0.3**	0.17	**0.32**	0.18	**0.32**	0.18	**0.31**	0.18
						2.50	**0.4**	0.23	**0.43**	0.25	**0.44**	0.25	**0.42**	0.24
						2.33	**0.45**	0.26	**0.48**	0.28	**0.47**	0.27	**0.47**	0.27
		7	8	1.4	0.369	3.00	**0.5**	0.36	**0.57**	0.41	**0.57**	0.41	**0.55**	0.39
						2.50	**0.62**	0.44	**0.68**	0.49	**0.69**	0.49	**0.66**	0.47
						2.33	**0.66**	0.47	**0.73**	0.52	**0.72**	0.51	**0.70**	0.50
		8	9	1.494	0.483	3.00	**0.39**	0.26	**0.43**	0.29	**0.44**	0.29	**0.42**	0.28
						2.50	**0.51**	0.34	**0.55**	0.37	**0.55**	0.37	**0.54**	0.36
						2.33	**0.55**	0.37	**0.6**	0.40	**0.58**	0.39	**0.58**	0.39
		9	60	1.593	0.659	3.00	**0.26**	0.16	**0.28**	0.18	**0.30**	0.19	**0.28**	0.18
						2.50	**0.36**	0.23	**0.38**	0.24	**0.39**	0.24	**0.38**	0.24
						2.33	**0.4**	0.25	**0.43**	0.27	**0.43**	0.27	**0.42**	0.26
	HP	1	61	1.676	0.613	3.00	**0.31**	0.18	**0.34**	0.20	**0.33**	0.20	**0.33**	0.19
						2.50	**0.42**	0.25	**0.45**	0.27	**0.45**	0.27	**0.44**	0.26
						2.33	**0.47**	0.28	**0.5**	0.30	**0.50**	0.30	**0.49**	0.29
		2	14	1.462	0.534	3.00	**0.33**	0.23	**0.37**	0.25	**0.36**	0.25	**0.35**	0.24
						2.50	**0.44**	0.30	**0.48**	0.33	**0.47**	0.32	**0.46**	0.32
						2.33	**0.48**	0.33	**0.52**	0.36	**0.52**	0.36	**0.51**	0.35
		3	18	2.241	0.922	3.00	**0.19**	0.08	**0.2**	0.09	**0.20**	0.09	**0.20**	0.09
						2.50	**0.29**	0.13	**0.3**	0.13	**0.31**	0.14	**0.30**	0.13
						2.33	**0.33**	0.15	**0.35**	0.16	**0.35**	0.16	**0.34**	0.15
		4	24	1.212	0.381	3.00	**0.42**	0.35	**0.48**	0.40	**0.46**	0.38	**0.45**	0.37

						2.50	**0.52**	0.43	**0.58**	0.48	**0.57**	0.47	**0.56**	0.46
						2.33	**0.56**	0.46	**0.62**	0.51	**0.62**	0.51	**0.60**	0.50
		5	9	1.845	0.447	3.00	**0.53**	0.29	**0.6**	0.33	**0.57**	0.31	**0.57**	0.31
						2.50	**0.68**	0.37	**0.74**	0.40	**0.74**	0.40	**0.72**	0.39
						2.33	**0.74**	0.40	**0.8**	0.43	**0.81**	0.44	**0.78**	0.42
		6	59	1.189	0.397	3.00	**0.39**	0.33	**0.45**	0.38	**0.44**	0.37	**0.43**	0.36
						2.50	**0.49**	0.41	**0.54**	0.45	**0.55**	0.46	**0.53**	0.44
						2.33	**0.53**	0.45	**0.58**	0.49	**0.58**	0.49	**0.56**	0.47
		7	11	1.401	0.297	3.00	**0.6**	0.43	**0.71**	0.51	**0.71**	0.51	**0.67**	0.48
						2.50	**0.72**	0.51	**0.82**	0.59	**0.83**	0.59	**0.79**	0.56
						2.33	**0.77**	0.55	**0.87**	0.62	**0.86**	0.61	**0.83**	0.59
		8	2	1.319	0.403	3.00	**0.43**	0.33	**0.49**	0.37	**0.50**	0.38	**0.47**	0.36
						2.50	**0.54**	0.41	**0.59**	0.45	**0.60**	0.45	**0.58**	0.44
						2.33	**0.58**	0.44	**0.64**	0.49	**0.64**	0.49	**0.62**	0.47
		9	111	1.216	0.753	3.00	**0.16**	0.13	**0.17**	0.14	**0.17**	0.14	**0.17**	0.14
						2.50	**0.22**	0.18	**0.24**	0.20	**0.24**	0.20	**0.23**	0.19
						2.33	**0.25**	0.21	**0.27**	0.22	**0.26**	0.21	**0.26**	0.21
	SPP	4	4	0.528	0.157	3.00	**0.31**	0.59	**0.4**	0.76	**0.40**	0.76	**0.37**	0.70
						2.50	**0.36**	0.68	**0.43**	0.81	**0.44**	0.83	**0.41**	0.78
						2.33	**0.37**	0.70	**0.45**	0.85	**0.45**	0.85	**0.42**	0.80
		5	2	0.49	0.455	3.00	**0.14**	0.29	**0.16**	0.33	**0.15**	0.31	**0.15**	0.31
						2.50	**0.18**	0.37	**0.19**	0.39	**0.19**	0.39	**0.19**	0.38
						2.33	**0.19**	0.39	**0.21**	0.43	**0.21**	0.43	**0.20**	0.41
		6	2	0.681	0.524	3.00	**0.16**	0.23	**0.18**	0.26	**0.18**	0.26	**0.17**	0.25
						2.50	**0.21**	0.31	**0.23**	0.34	**0.22**	0.32	**0.22**	0.32
						2.33	**0.23**	0.34	**0.25**	0.37	**0.25**	0.37	**0.24**	0.36
		9	12	0.555	0.427	3.00	**0.17**	0.31	**0.19**	0.34	**0.19**	0.34	**0.18**	0.33
						2.50	**0.21**	0.38	**0.24**	0.43	**0.23**	0.41	**0.23**	0.41
						2.33	**0.23**	0.41	**0.26**	0.47	**0.25**	0.45	**0.25**	0.44
PDA	PSC	1	41	1.369	0.925	3.00	**0.12**	0.09	**0.12**	0.09	**0.12**	0.09	**0.12**	0.09
						2.50	**0.17**	0.12	**0.18**	0.13	**0.18**	0.13	**0.18**	0.13
						2.33	**0.2**	0.15	**0.21**	0.15	**0.21**	0.15	**0.21**	0.15
		2	5	1.342	0.262	3.00	**0.63**	0.47	**0.75**	0.56	**0.75**	0.56	**0.71**	0.53
						2.50	**0.74**	0.55	**0.86**	0.64	**0.85**	0.63	**0.82**	0.61
						2.33	**0.79**	0.59	**0.9**	0.67	**0.90**	0.67	**0.86**	0.64
		3	26	1.702	0.566	3.00	**0.36**	0.21	**0.39**	0.23	**0.40**	0.24	**0.38**	0.23
						2.50	**0.48**	0.28	**0.51**	0.30	**0.51**	0.30	**0.50**	0.29
						2.33	**0.52**	0.31	**0.56**	0.33	**0.57**	0.33	**0.55**	0.32
		4	25	1.584	0.617	3.00	**0.29**	0.18	**0.32**	0.20	**0.32**	0.20	**0.31**	0.20
						2.50	**0.39**	0.25	**0.42**	0.27	**0.42**	0.27	**0.41**	0.26
						2.33	**0.44**	0.28	**0.46**	0.29	**0.46**	0.29	**0.45**	0.29
		5	17	1.315	0.395	3.00	**0.44**	0.33	**0.5**	0.38	**0.48**	0.37	**0.47**	0.36
						2.50	**0.55**	0.42	**0.6**	0.46	**0.61**	0.46	**0.59**	0.45
						2.33	**0.59**	0.45	**0.65**	0.49	**0.65**	0.49	**0.63**	0.48
		6	47	1.716	0.555	3.00	**0.37**	0.22	**0.41**	0.24	**0.42**	0.24	**0.40**	0.23
						2.50	**0.49**	0.29	**0.53**	0.31	**0.53**	0.31	**0.52**	0.30
						2.33	**0.54**	0.31	**0.58**	0.34	**0.57**	0.33	**0.56**	0.33
		7	8	1.443	0.398	3.00	**0.48**	0.33	**0.54**	0.37	**0.54**	0.37	**0.52**	0.36
						2.50	**0.59**	0.41	**0.66**	0.46	**0.65**	0.45	**0.63**	0.44
						2.33	**0.64**	0.44	**0.7**	0.49	**0.70**	0.49	**0.68**	0.47
		8	9	1.525	0.413	3.00	**0.48**	0.31	**0.55**	0.36	**0.52**	0.34	**0.52**	0.34
						2.50	**0.61**	0.40	**0.67**	0.44	**0.66**	0.43	**0.65**	0.42
						2.33	**0.66**	0.43	**0.72**	0.47	**0.72**	0.47	**0.70**	0.46
		9	61	1.643	0.644	3.00	**0.28**	0.17	**0.3**	0.18	**0.30**	0.18	**0.29**	0.18

						2.50	**0.38**	0.23	**0.41**	0.25	**0.41**	0.25	**0.40**	0.24
						2.33	**0.43**	0.26	**0.46**	0.28	**0.45**	0.27	**0.45**	0.27
	HP	1	65	1.79	0.528	3.00	**0.42**	0.23	**0.46**	0.26	**0.45**	0.25	**0.44**	0.25
						2.50	**0.55**	0.31	**0.59**	0.33	**0.59**	0.33	**0.58**	0.32
						2.33	**0.6**	0.34	**0.64**	0.36	**0.65**	0.36	**0.63**	0.35
		2	14	1.631	0.481	3.00	**0.43**	0.26	**0.48**	0.29	**0.48**	0.29	**0.46**	0.28
						2.50	**0.55**	0.34	**0.6**	0.37	**0.60**	0.37	**0.58**	0.36
						2.33	**0.6**	0.37	**0.65**	0.40	**0.65**	0.40	**0.63**	0.39
		3	18	2.406	0.868	3.00	**0.23**	0.10	**0.25**	0.10	**0.25**	0.10	**0.24**	0.10
						2.50	**0.35**	0.15	**0.36**	0.15	**0.36**	0.15	**0.36**	0.15
						2.33	**0.39**	0.16	**0.41**	0.17	**0.41**	0.17	**0.40**	0.17
		4	24	1.369	0.410	3.00	**0.44**	0.32	**0.49**	0.36	**0.49**	0.36	**0.47**	0.35
						2.50	**0.55**	0.40	**0.61**	0.45	**0.62**	0.45	**0.59**	0.43
						2.33	**0.59**	0.43	**0.65**	0.47	**0.65**	0.47	**0.63**	0.46
		5	9	1.995	0.438	3.00	**0.59**	0.30	**0.66**	0.33	**0.67**	0.34	**0.64**	0.32
						2.50	**0.75**	0.38	**0.82**	0.41	**0.82**	0.41	**0.80**	0.40
						2.33	**0.81**	0.41	**0.88**	0.44	**0.89**	0.45	**0.86**	0.43
		6	59	1.292	0.363	3.00	**0.47**	0.36	**0.53**	0.41	**0.52**	0.40	**0.51**	0.39
						2.50	**0.58**	0.45	**0.64**	0.50	**0.65**	0.50	**0.62**	0.48
						2.33	**0.62**	0.48	**0.68**	0.53	**0.68**	0.53	**0.66**	0.51
		7	11	1.489	0.327	3.00	**0.59**	0.40	**0.69**	0.46	**0.70**	0.47	**0.66**	0.44
						2.50	**0.72**	0.48	**0.81**	0.54	**0.82**	0.55	**0.78**	0.53
						2.33	**0.77**	0.52	**0.86**	0.58	**0.87**	0.58	**0.83**	0.56
		8	2	1.354	0.415	3.00	**0.43**	0.32	**0.48**	0.35	**0.48**	0.35	**0.46**	0.34
						2.50	**0.54**	0.40	**0.59**	0.44	**0.59**	0.44	**0.57**	0.42
						2.33	**0.58**	0.43	**0.64**	0.47	**0.64**	0.47	**0.62**	0.46
		9	110	1.35	0.676	3.00	**0.21**	0.16	**0.23**	0.17	**0.23**	0.17	**0.22**	0.17
						2.50	**0.29**	0.21	**0.31**	0.23	**0.30**	0.22	**0.30**	0.22
						2.33	**0.33**	0.24	**0.35**	0.26	**0.35**	0.26	**0.34**	0.25
	SPP	4	4	0.664	0.014	3.00	**0.46**	0.69	**0.7**	1.05	**0.65**	0.98	**0.60**	0.91
						2.50	**0.51**	0.77	**0.69**	1.04	**0.69**	1.04	**0.63**	0.95
						2.33	**0.53**	0.80	**0.65**	0.98	**0.70**	1.05	**0.63**	0.94
		5	2	0.661	0.440	3.00	**0.19**	0.29	**0.22**	0.33	**0.22**	0.33	**0.21**	0.32
						2.50	**0.25**	0.38	**0.27**	0.41	**0.27**	0.41	**0.26**	0.40
						2.33	**0.27**	0.41	**0.29**	0.44	**0.29**	0.44	**0.28**	0.43
		6	2	1.239	0.320	3.00	**0.5**	0.40	**0.58**	0.47	**0.59**	0.48	**0.56**	0.45
						2.50	**0.61**	0.49	**0.69**	0.56	**0.70**	0.56	**0.67**	0.54
						2.33	**0.65**	0.52	**0.73**	0.59	**0.73**	0.59	**0.70**	0.57
		9	12	0.682	0.293	3.00	**0.3**	0.44	**0.35**	0.51	**0.35**	0.51	**0.33**	0.49
						2.50	**0.35**	0.51	**0.4**	0.59	**0.40**	0.59	**0.38**	0.56
						2.33	**0.38**	0.56	**0.43**	0.63	**0.43**	0.63	**0.41**	0.61

Table 13: Preliminary resistance factors for Data Case D

Design Method	Soil Regions	# of Piles	Mean (λ_R)	COV_R	β	FOSM		FORM		MC		Average	
						φ_R	φ_R/λ	φ_R	φ_R/λ	φ_R	φ_R/λ	φ_R	φ_R/λ
CAPWAP	Quaternary	191	1.385	0.544	3.00	**0.31**	0.22	**0.34**	0.25	**0.33**	0.24	**0.33**	0.24
					2.50	**0.41**	0.30	**0.44**	0.32	**0.44**	0.32	**0.43**	0.31
					2.33	**0.45**	0.32	**0.48**	0.35	**0.48**	0.35	**0.47**	0.34
	Tertiary All	336	1.716	0.775	3.00	**0.21**	0.12	**0.22**	0.13	**0.21**	0.12	**0.21**	0.12
					2.50	**0.3**	0.17	**0.32**	0.19	**0.33**	0.19	**0.32**	0.18
					2.33	**0.34**	0.20	**0.36**	0.21	**0.35**	0.20	**0.35**	0.20

	Tertiary, Soil profile codes: 1-4-7	130	1.596	0.565	3.00	**0.34**	0.21	**0.37**	0.23	**0.37**	0.23	**0.36**	0.23
					2.50	**0.45**	0.28	**0.48**	0.30	**0.49**	0.31	**0.47**	0.30
					2.33	**0.49**	0.31	**0.53**	0.33	**0.54**	0.34	**0.52**	0.33
	Tertiary, Soil profile codes: 3-6-9	150	1.532	0.846	3.00	**0.16**	0.10	**0.17**	0.11	**0.17**	0.11	**0.17**	0.10
					2.50	**0.23**	0.14	**0.24**	0.15	**0.25**	0.16	**0.24**	0.15
					2.33	**0.26**	0.16	**0.28**	0.18	**0.27**	0.17	**0.27**	0.17
	Cretaceous	38	1.196	0.347	3.00	**0.45**	0.28	**0.52**	0.33	**0.52**	0.33	**0.50**	0.31
					2.50	**0.55**	0.34	**0.62**	0.39	**0.62**	0.39	**0.60**	0.37
					2.33	**0.59**	0.37	**0.66**	0.41	**0.66**	0.41	**0.64**	0.40
PDA	Quaternary	192	1.49	0.491	3.00	**0.38**	0.26	**0.42**	0.28	**0.42**	0.28	**0.41**	0.27
					2.50	**0.49**	0.33	**0.54**	0.36	**0.54**	0.36	**0.52**	0.35
					2.33	**0.54**	0.36	**0.58**	0.39	**0.58**	0.39	**0.57**	0.38
	Tertiary	339	1.78	0.737	3.00	**0.24**	0.13	**0.26**	0.15	**0.26**	0.15	**0.25**	0.14
					2.50	**0.34**	0.19	**0.36**	0.20	**0.35**	0.20	**0.35**	0.20
					2.33	**0.38**	0.21	**0.4**	0.22	**0.41**	0.23	**0.40**	0.22
	Tertiary, Soil profile codes: 1-4-7	134	1.662	0.525	3.00	**0.39**	0.23	**0.43**	0.26	**0.43**	0.26	**0.42**	0.25
					2.50	**0.51**	0.31	**0.55**	0.33	**0.55**	0.33	**0.54**	0.32
					2.33	**0.56**	0.34	**0.6**	0.36	**0.6**	0.36	**0.59**	0.35
	Tertiary, Soil profile codes: 3-6-9	149	1.602	0.788	3.00	**0.19**	0.11	**0.2**	0.12	**0.2**	0.12	**0.20**	0.12
					2.50	**0.27**	0.16	**0.29**	0.17	**0.29**	0.17	**0.28**	0.17
					2.33	**0.31**	0.19	**0.32**	0.19	**0.32**	0.19	**0.32**	0.19
	Cretaceous	38	1.274	0.344	3.00	**0.49**	0.29	**0.56**	0.34	**0.56**	0.34	**0.54**	0.32
					2.50	**0.59**	0.35	**0.66**	0.40	**0.66**	0.40	**0.64**	0.38
					2.33	**0.63**	0.38	**0.71**	0.43	**0.34**	0.20	**0.56**	0.34

Tables 10 to 13 reveal that the data Case A presents the most conservative method concerning resistance factor, with an average resistance factor of 0.33 and an average efficiency factor of 0.28. The data Case B shows an average resistance factor of 0.45 and an average efficiency factor of 0.31, representing a 36% and 11% increase from data Case A results, respectively. The data Case C shows an average resistance factor of 0.48 and an average efficiency factor of 0.38, representing a 45% and a 36% increase from data Case A results, respectively. The data Case D shows an average resistance factor of 0.41 and an average efficiency factor of 0.26, representing a 24% increase and an 8% decrease from data Case A results, respectively.

When the data is categorized by pile material and soil type, as shown in Case C, an average resistance factor of 0.48 represents a 45% increment concerning the resistance factors calibrated when just pile type (Case A) is considered (0.33). These results also confirm that the more specific the categorization, the less external variables affect the results; therefore, higher resistance factors occur.

Data Case A is used to compare the results from calibration methods FOSM, FORM, and MCS because it presents the most conservative method concerning resistance factor. Figure 12

shows a comparison of the resistance factor between FOSM and FORM, Figure 13 shows a comparison of the resistance factor between FOSM and MCS, and Figure 14 shows a comparison of the resistance factor between FORM and MCS.

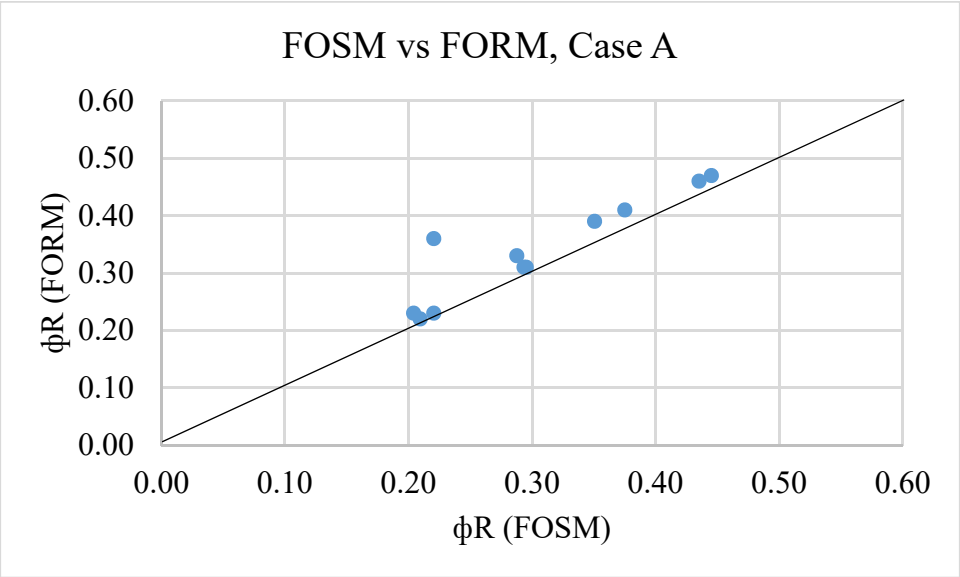

Figure 12: FOSM vs FORM results, Case A.

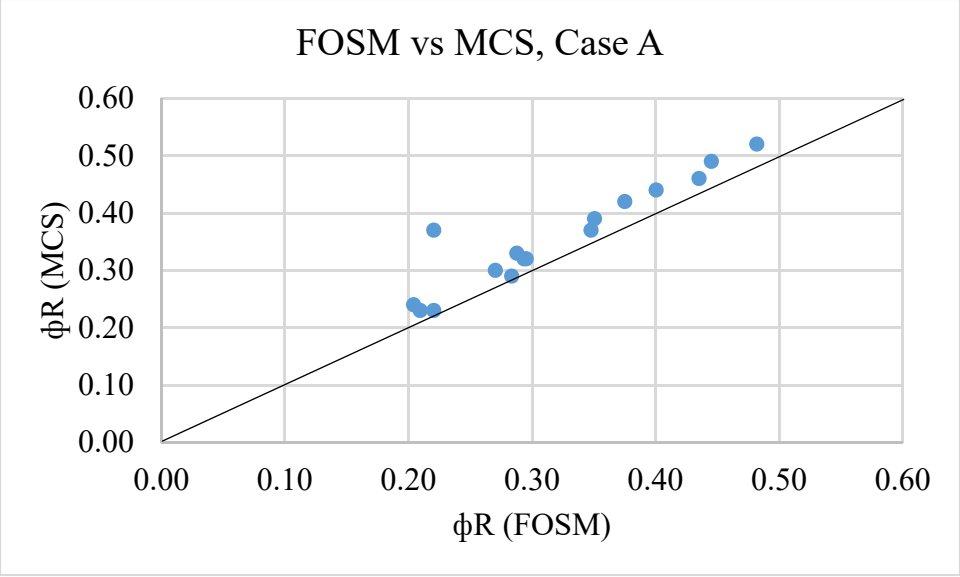

Figure 13: FOSM vs MCS results, Case A.

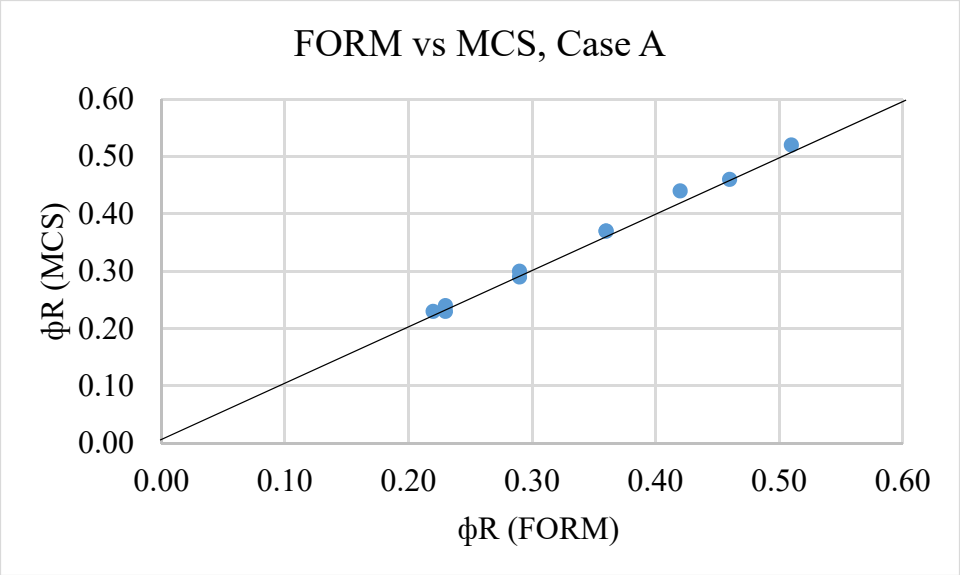

Figure 14: FORM vs MCS results, Case A.

When comparing FOSM, FORM, and MCS results from data Case A, Table 10 and Figures 11 to 13 show that FORM produces 6.5% higher resistance factors than FOSM on average, MCS produces 9.7% higher than FOSM on average. MCS produces 3% higher resistance factors than FORM on average. Therefore, it can be concluded that FOSM is the most conservative calibration method, while MCS is the least most conservative calibration method.

4.2 Estimating Pile Setup Factors

According to Haque and Steward [24], the incorporation of pile setup in the design stage would produce meaningful construction cost savings. As stated in Chapter 2, pile setup represents an increase on the pile capacity over time after the EOID. Larger pile capacity can be translated to smaller piles size, depth and number. These three factors represent less construction costs to the government and taxpayers.

The most popular empirical model to predict pile setup behavior is developed by Skov and Denver [1] due to its simplicity. This study utilized the following equation to compute the setup parameter (log-linear) A:

$$\frac{R_t}{R_{to}} = A\, log_{10}\frac{t}{t_o} + 1, \tag{69}$$

where t_o of 15 minutes was used as the initial reference time for all the calculations, which is the value used and recommended in the study presented by Haque and Steward [24]. The other values utilized for computing setup parameter are part of the database obtained from the CAPWAP dynamic load test measurements. The parameter A depends on the soil type, pile material, pile type, pile size, and pile capacity [24].

To compute an average setup factor for this study's database, the data categorization was first developed based on the actual pile information for the time after EOID. The piles with restrikes after EOID greater than one day was accounted for the setup factor computation of the total pile resistance. Thirty-nine piles were used for the calculation, 8 PSC, 22 HP, and 9 PSS pile types. Table 14 and Figure 15 show the summary results obtained from the different types of pile groups used for the setup factor computation. While Table 15 and Figure 16 show the summary results obtained from the different soil profiles group. Only 35 piles had enough information available about soil profiles. The study results presented in this section utilize the data obtained from the CAPWAP dynamic load test measurements

Table 14: Summary of average results for piles setup factor with time after EOID greater than a day based on pile material type.

Design Method	Material type	# of piles	Time intervals (days)	Δ Emb. Length (ft)	Rt/Rto	Setup factor A
APILE	All	39	5	0.5	2.59	**0.78**
	PSC	8	3	0.3	6.07	**2.55**
	HP	22	5	0.2	1.64	**0.30**
	SPP	9	6	1.2	1.82	**0.40**

Table 15: Summary of average results for piles setup factor with time after EOID greater than a day based on soil profile.

Design Method	Soil profile	Soil along shaft	Soil at toe	# of piles	Time intervals (days)	Δ Emb. Length (ft)	Setup factor A
APILE	1	Clay	Clay	3	3	0.4	**0.31**
	4	Mixed	Clay	5	4	0.1	**0.62**
	5	Mixed	Mixed	2	5	0.0	**0.24**
	6	Mixed	Sand	8	6	0.2	**2.63**

	7	Sand	Clay	1	7	0.1	**0.33**
	9	Sand	Sand	16	5	0.8	**0.26**

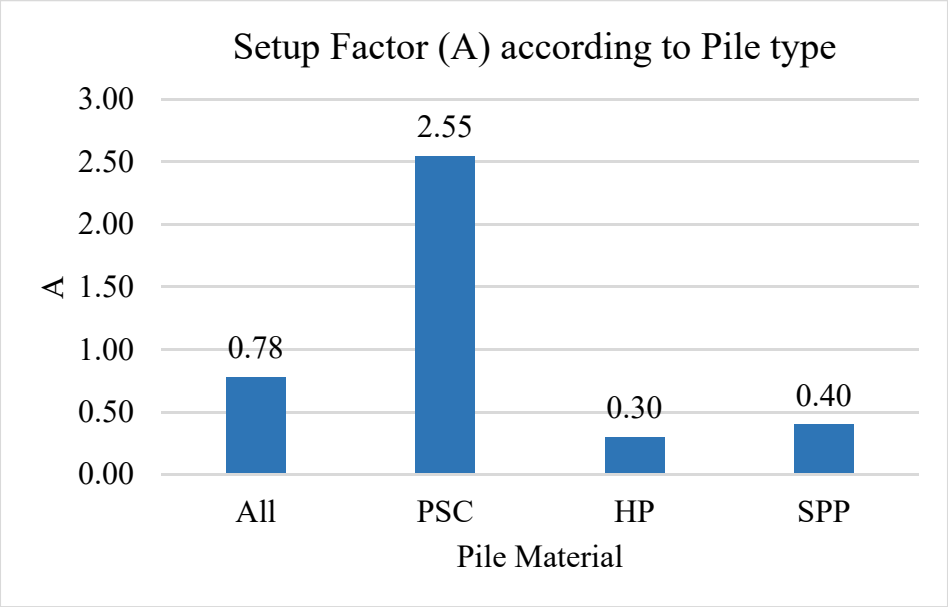

Figure 15: Setup factor average results according to pile type.

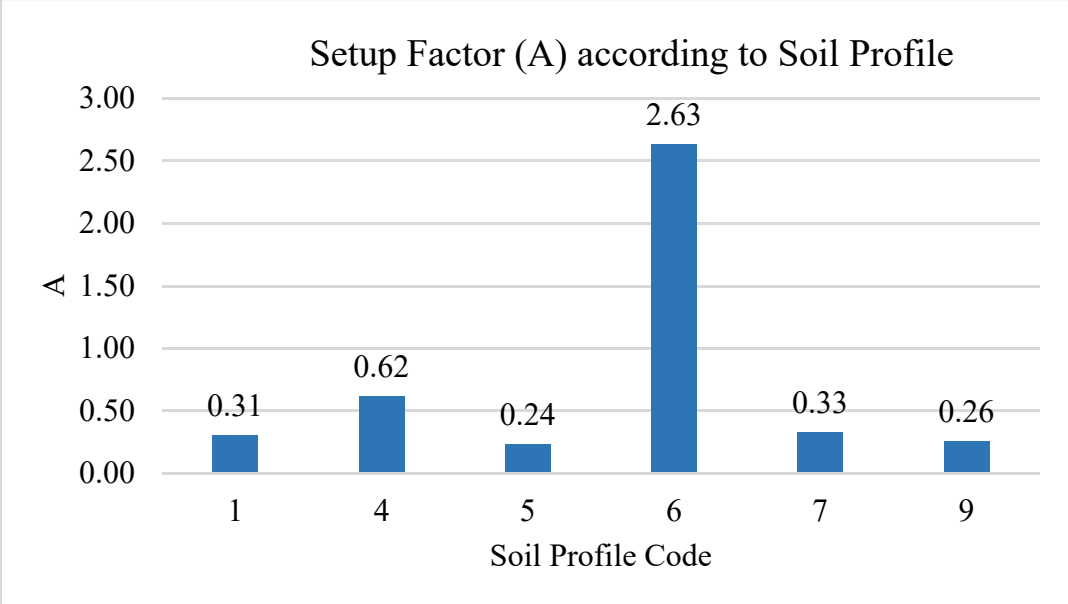

Figure 16: Setup factor average results according to soil category.

Figure 15 shows that the lowest setup factor of 0.30 belongs to the HP piles group regarding the setup factor results. PSC piles show the highest factor of 2.55, representing an 850% increase from the HP piles result. At the same time, the SPP group with a setup factor of 0.40 and all piles group (0.78) values are located in between the highest and lowest factors computed. It can also be concluded that when the different groups of piles material are combined, the setup factor computed is the second highest factor in the results.

When the data is divided based on soil profile, Figure 16 shows that the type of soil 6 has the highest setup factor of 2.63, while the lowest factor of 0.24 is found in soil type 5. Even though there is no a clear trend, it can be observed from Table 15 that when the time interval is the same (5 days), the setup factor is slightly close and only differ by 8%.

The setup factor analysis for the dataset categorized by soil regions (Case D) was also performed in this study. Table 16 and Figure 17 show the setup factor results, and detailed information of the number of piles used in each subgroup.

Table 16: Summary of average results for piles setup factor with time after EOID greater than a day based on soil region.

Design Method	Soil Region	# of piles	Time intervals (days)	Setup Factor
APILE	Quaternary	5	5	0.24
	Tertiary	17	4	0.32
	Tertiary 1-4-7	5	4	0.62
	Tertiary 3-6-9	10	5	0.18
	Cretaceous	0	0	N/A

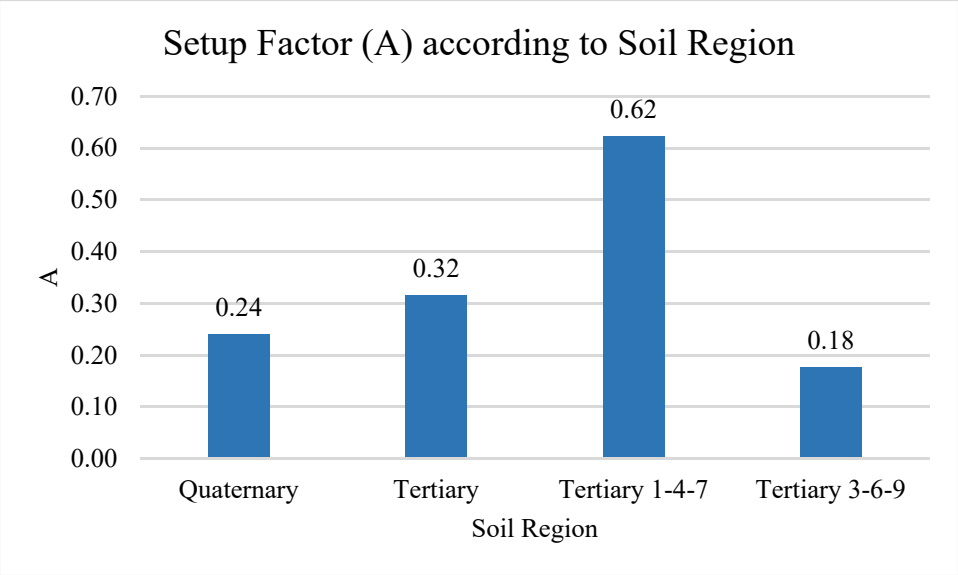

Figure 17: Setup factor average results according to soil region.

Regarding the total resistance of piles, it was observed in Figure 17 that the Tertiary 1-4-7 group has the largest setup factor of 0.62. It was also found that there is a considerable difference between the setup factors for Tertiary 1-4-7 and Tertiary 3-6-9. Tertiary 1-4-7 shows a setup factor 94% larger than the one for Tertiary 3-6-9. These results also explain why, once the Tertiary data is grouped in a single set, it shows small consistency. The Quaternary group shows a setup factor of 0.24, which was very consistent even with a small data size of 5 piles.

4.3 Comparison of Resistance Factors.

In this section, the results of the Mississippi DOT resistance factors are evaluated by comparing with published data from the AASHTO Bridge Design Manual [28] and NCHRP 507 Driving pile manual [5] and the neighboring state of Alabama, which the authors have specific experience with. The study results presented in this section utilize the resistance factors obtained from the CAPWAP dynamic load test measurements. It should be noted that, as seen in this section, specific comparisons are difficult due to the variations in the data collected by each study, specifically, that there are no static load test data within the MDOT database. Further, while other documents consider the soil type factor, this document considers the type of pile due

to the lack of data in specific soil types. Nevertheless, the comparison developed is useful to evaluate the performance of the prediction method used in this study.

4.3.1 Comparison of Resistance Factor results with AASHTO.

This section compares the resistance factors obtained in this study with the resistance factors provided by the AASHTO [14] specifications. AASHTO presents resistance factors for static analysis methods that is considered comparable to the measured analysis used in MDOT analysis. In regard of static analysis methods, AASHTO mainly considered the resistance factors calibrated by Paikowsky et al. [5]. However, since several resistance factors were calibrated, AASHTO [14] lists the average resistance factors for each method. It should be noted that AASHTO lists resistance factors for redundant piles. Nonetheless, its commentary suggests using 80% of the redundant resistance factors for non-redundant piles.

A comparison between the study's resistance factors and the resistance factors proposed by AASHTO [14] is shown in Table 17.

Table 17: Comparison of the MDOT resistance factors with AASHTO specifications.

	Mississippi				AASHTO					
Year	2020				2014					
Pile Type	All Piles	PSC	HP	SPP	Side and End bearing resistance: Clay and Mixed Soils			Side and End bearing resistance: Sand		General
Design method	APILE	APILE	APILE	APILE	α	β	λ	Nordlund/ Thurman	SPT	Schmertmann (CPT)
φ (β = 2.33)	**0.34**	**0.47**	**0.29**	**0.29**	**0.35**	**0.25**	**0.40**	**0.45**	**0.30**	**0.50**
φ (β = 3.00)	**0.22**	**0.31**	**0.18**	**0.22**	**0.28**	**0.20**	**0.32**	**0.36**	**0.24**	**0.40**

MDOT's resistance factors are similar or in some groups higher to AASHTO's resistance factors for the α, β, λ, and SPT methods. Nevertheless, MDOT's resistance factors are slightly

lower than AASHTO's resistance factors from the Nordlund/Thurman and the Schmertmann (CPT) method, except the PSC group for redundant piles that presents a higher resistance factor than the Nordlund/Thurman. The slight difference between the resistance factors of MDOT and AASHTO can be attributed to the fact that this study utilized specific data from the state of Mississippi, and AASHTO utilized a database from throughout the United States.

4.3.2 Comparison of Resistance Factors with NCHRP 507

This section compares the resistance factors from this study with the resistance factors provided by the report 507 from NCHRP[5]. The NCHRP 507 [5] specifications is a document developed by Paikowsky et al. in order to address issues with the original AASHTO report and to provide resistance factors for the design of various deep foundation systems. In the case of driven piles, the database is composed of 338 static analysis case histories and 210 static and dynamic tested cases. The calibration methodology used is FOSM and FORM with 2.33 and 3.0 as reliability indices. All of the suggested resistance factors developed with for target reliability values can be found in the Tables 25 – 30 of NCHRP 507 [5] report.

NCHRP 507 [5] states that static capacity design methods tend to over-predict the capacity of observed pile capacities. On the other hand, dynamic capacity evaluation methods usually used for control tend to under-predict the observed pile capacities. It should be noted that parameters such as subsurface variability, site-specific technology, and previous experience, as well as amount and type of testing during construction, were not considered for this study.

Several resistance factors were calibrated by Paikowsky et al. [5] in NCHRP 507. However, Tables 18, 19 and 20 show the comparison of the resistance factors from Mississippi with the resistance factors calibrated using FORM and dead-to-live load ratio of 2. Table 18 shows the comparison for the PSC piles, Table 19 shows the comparison for the HP group, and Table 20 shows the comparison for SPP group.

Table 18: Comparison of the resistance factors from MDOT with the resistance factors from NCHRP 507 (PSC).

State		Mississippi (2020)		NCHRP 507	
Case w/o Pile Type		All Piles	PSC	Concrete Pile (Mixed soils)	
Design method		APILE	APILE	β-method/ Thurman	αTomlinson/ Norlund/ Thurman
Data set size		648	279	80	33
λ_R		1.499	1.651	0.810	0.960
COV_R		0.726	0.633	0.380	0.490
φ_R	β = 2.33	**0.34**	**0.47**	**0.40**	**0.40**
φ_R/λ_R		0.23	0.28	0.49	0.42
φ_R	β = 3.00	**0.22**	**0.21**	**0.30**	**0.30**
φ_R/λ_R		0.15	0.19	0.37	0.31

Table 19: Comparison of the resistance factors from MDOT with the resistance factors from NCHRP 507 (HP).

State		Mississippi (2020)		NCHRP 507	
Case w/o Pile Type		All Piles	HP	HP (Mixed soils)	
Design method		APILE	APILE	α-API/ Norlund/ Thurmand	αTomlinson/ Norlund/ Thurman
Data set size		648	347	34	20
λ_R		1.499	1.437	0.790	0.590
COV_R		0.726	0.782	0.440	0.390
φ_R	β = 2.33	**0.34**	**0.29**	**0.35**	**0.30**
φ_R/λ_R		0.23	0.20	0.44	0.51
φ_R	β = 3.00	**0.22**	**0.18**	**0.25**	**0.25**
φ_R/λ_R		0.15	0.13	0.32	0.42

Table 20: Comparison of the resistance factors from MDOT with the resistance factors from NCHRP 507 (SPP).

State		Mississippi (2020)		NCHRP 507	
Case w/o Pile Type		All Piles	SPP	SPP (Mixed soils)	
Design method		APILE	APILE	β-method/ Thurman	αTomlinson/ Norlund/ Thurman
Data set size		648	22	29	13
λ_R		1.499	0.564	0.540	0.740
COV_R		0.726	0.368	0.480	0.590
φ_R	β = 2.33	**0.34**	**0.29**	**0.25**	**0.25**
φ_R/λ_R		0.23	0.40	0.46	0.34
φ_R	β = 3.00	**0.22**	**0.22**	**0.15**	**0.15**
φ_R/λ_R		0.15	0.51	0.28	0.20

In general, MDOT's results show similar resistance factors compared to NCHRP's static analysis methods. Regarding PSC piles, MDOT's results offer higher resistance factors than NCHRP for redundant piles. For HP piles, MDOT's resistance factors are slightly lower than NCHRP's resistance factors for redundant and non-redundant piles. On the other hand, for the SPP group, MDOT's resistance factors are higher than NCHRP's resistance factors for all the presented cases. MDOT offers slightly lower resistance factors regarding all piles case, except for when they are compared to the SPP group, where MDOT has higher resistance factors than NCHRP.

According to the LRFD calibration performed in this study, the resistance factors obtained from the MDOT's database are similar to the recommended resistance factors presented in the NCHRP report. MDOT's resistance factors should be considered over the other methods, considering the NCHRP study is based on a database from different states.

4.3.3 Comparison of Resistance Factors with the State of Alabama.

This section attempt to compare the resistance factors obtained in this study with a study presented by Steward and Cleary [41]. The ALDOT study calibrated LRFD resistance factors using the First Order Second Moment (FOSM), First Order Reliability Method (FORM), and Monte Carlo Simulation (MCS) in Alabama soils. The target reliability index used in the ALDOT study is the same as presented in this study. The ALDOT study [41] is mostly composed of a dataset with only static load test information. It should be noted that Alabama does not have SPP type of piles, while Mississippi dataset has a total of 22 SPP type.

Table 21 shows the comparison of the resistance factors from Mississippi with the recommended resistance factors presented in the ALDOT's study.

Table 21: Comparison of the resistance factors from MDOT with the resistance factors from the state of Alabama.

State		Mississippi (2020)			Alabama (2020)		
Case w/o Pile Type		All Piles	PSC	HP	All Piles	Concrete Piles	Steel H-piles
Design method		APILE	APILE	APILE	DRIVEN	DRIVEN	DRIVEN
Number of Piles		648	276	347	53	17	36
φ_R	β = 2.33	**0.34**	**0.47**	**0.29**	**0.22**	**0.25**	**0.28**
φ/λ		0.23	0.28	0.20	0.21	0.38	0.23
φ_R	β = 3.00	**0.22**	**0.31**	**0.18**	**0.14**	**0.17**	**0.20**
φ/λ		0.15	0.19	0.13	0.13	0.26	0.16

According to Table 21, Alabama design method has lower resistance factors than MDOT's design method for redundant and non-redundant piles, except for the HP group, where Alabama study offers a higher resistance factor than MDOT's study. The difference found in the comparison of Table 21 may be due to the significant difference in the database's size. In terms of efficiency, Alabama presents a higher average efficiency factor of 0.7 for non-redundant piles and 0.18 for redundant piles than this study.

4.3.4 Summary of MDOT Resistance Factors compared to AASHTO, NCHRP 507, and the State of Alabama.

This section attempts to summarize the comparison of the performance of the prediction method used by MDOT with design methods used by the federal government and the neighboring state of Alabama. The group of piles with the highest MDOT resistance factor is compared with the highest resistance factors obtained from the comparisons presented in the previous sections.

According to the comparison performed, MDOT's resistance factors are similar, or in some cases, higher than the resistance factors provide by AASHTO and NCHRP 507. Also, this similarity remains for the state of Alabama. Therefore, it can be concluded that utilizing these new calibrated resistance factors from this study would provide improved accuracy because this study uses local test data. For a better appreciation, Figures 18 and 19 show a comparison of the highest MDOT's resistance factor with the static analysis methods with the highest resistance factors found in this section for redundant and non-redundant piles.

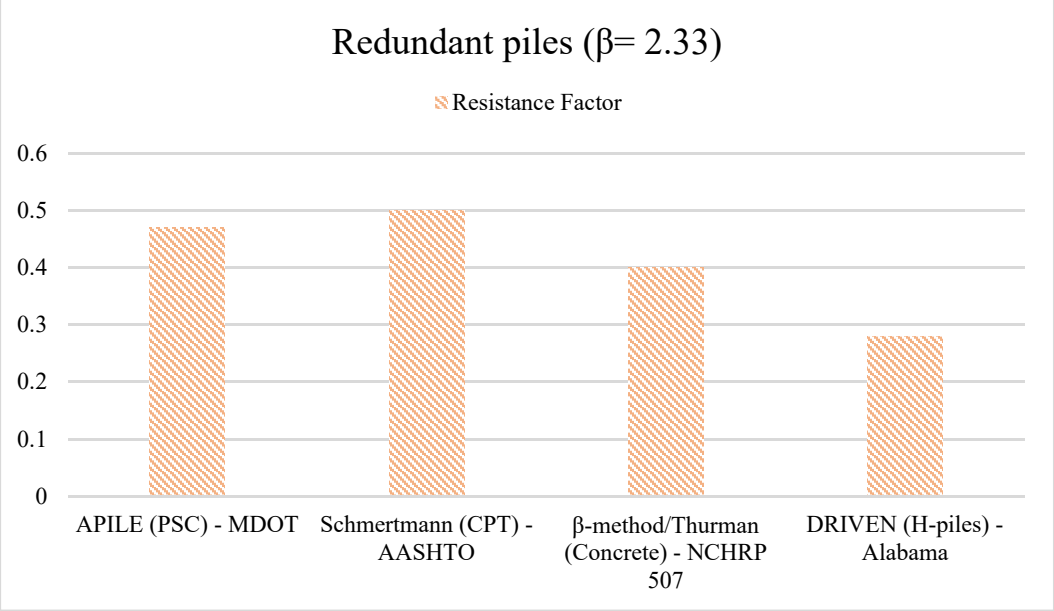

Figure 18: Static analysis methods with the highest resistance factors for redundant piles.

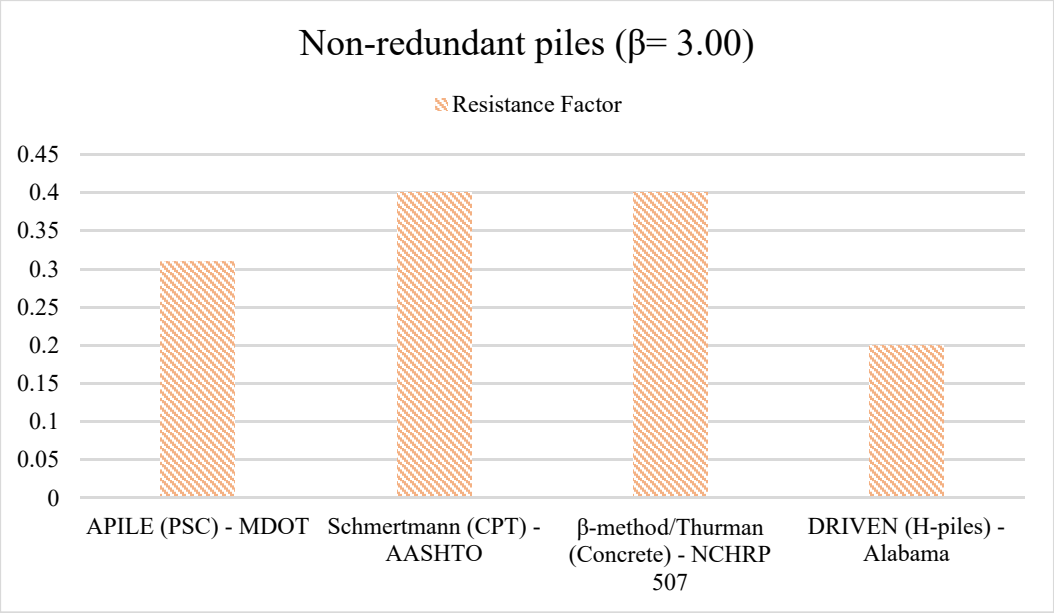

Figure 19: Static analysis methods with the highest resistance factors for non-redundant piles.

Figure 18 shows that, concerning redundant piles, the PSC pile group for MDOT has a similar resistance factor to the highest resistance factor using the Schmertmann method presented by AASHTO. Figure 19 shows that, concerning non-redundant piles, the resistance factors presented by AASHTO and NCHRP 507 are higher than the resistance factor for MDOT's study.

CHAPTER V - CONCLUSIONS

The main objective of this study is to develop LRFD resistance factors unique to Mississippi soils using FOSM, FORM, and MCS, in order to enhance accuracy and efficiency of pile design. The second objective is to developed pile setup factors in different datasets. Finally, the third objective is to compare the calibrated resistance factors with the recommended resistance factors from published studies from the federal government and the state of Alabama. The conclusions obtained from these objectives and analysis are described in the following paragraphs.

According to the data provided by MDOT and the evaluation of the performance of the measured methods of CAPWAP and PDA capacities, PDA predicts a 20% higher pile capacity than CAPWAP on average. Results reveal that the data Case A (type of pile) presented the most conservative method concerning resistance and efficiency factors. The dataset for Prestress concrete piles offered the highest resistance and efficiency factors compared to the other pile types of Case A. Furthermore, in Case B (soil type), the measured method of CAPWAP predicted the highest resistance factor on average in soil type 7, sand along the shaft and clay at the toe of the pile, which is 182% higher than the lowest resistance factor predicted in soil type 9, sand along the shaft and sand at the toe of the pile. The data Case C has the highest average resistance factor of 0.48 and an average efficiency factor of 0.38, representing a 45% and a 36% increase from data Case A results, respectively. When the data is categorized by pile material and soil type, as presented in Case C, the results confirm that the more specific the categorization, the less external variables affect the results; therefore, higher resistance factors.

Data Case A is used to compare the results from calibration methods FOSM, FORM, and MCS because it presented the most conservative method concerning resistance factor. The comparison shows that the FOSM method produced the lowest resistance factors on average than the other two methods. MCS produced 9.7% higher resistance factors than FOSM on average. Therefore, from the three calibration methods utilized, MCS produced the largest resistance factors on average.

The procedure of computing an average setup factor for this study is based on the time after EOID. The piles with enough data with time after EOID greater than one day are accounted for the setup factors computation. The results showed the lowest setup factor of 0.30 belongs to

the HP piles group, while PSC piles group had the highest factor of 2.55. When the different groups of pile materials are combined (all piles) the setup factor computed is the second highest factor in the results. When the database is divided based on soil profile, the type of soil 6 had the highest setup factor of 2.63, while the lowest factor of 0.24 is found in soil type 5.

The setup factor analysis for the dataset categorized by soil regions (Case D) is also performed in this study. The largest setup factor of 0.62 was found in the Tertiary 1-4-7 group. Also, it is concluded that a considerable difference of 94% for the setup factors computed for the Tertiary groups is observed. The Quaternary group has a setup factor of 0.24, which is very consistent even with a small data size of 5 piles.

According to the comparison performed, MDOT's resistance factors are similar, or in some cases, higher than the resistance factors provide by the AASHTO and NCHRP 507. MDOT's resistance factors are also similar to the resistance factors presented in a recent study within the state of Alabama. Therefore, it is concluded based on average that the design method used by MDOT is more efficient and accurate than the design methods presented by the nationally published studies due to the regional nature of the dataset utilized.

According to the data provided by MDOT and the calibration performed, it is concluded to consider the results of the Monte Carlo calibration method with the CAPWAP dynamic load test measurements, and the data Case A, which includes all data available, as the definitive resistance factors. The final recommended resistance factors for Mississippi are shown in Table 22. The resistance factors from AASHTO specifications [14] are also listed in Table 22 to show whether this study calibrated higher or lower resistance factors.

Table 22: Recommended resistance factors for driven piles in the state of Mississippi

Condition	Pile Type	Prediction Method	Resistance factor ϕR	ϕR from AASHTO (2014)
Nominal axial bearing resistance of non-redundant pile (4 piles or less)	All Piles	APILE	**0.23**	0.36 or 0.28
	PSC		**0.32**	
	HP		**0.19**	
	SPP		**0.24**	
Nominal axial bearing resistance of redundant pile (5 piles or more)	All Piles	APILE	**0.35**	0.45 or 0.35
	PSC		**0.49**	
	HP		**0.29**	
	SPP		**0.30**	

CHAPTER VI – RECOMMENDATIONS

The purpose of this study was to determine the regionally calibrated resistance factors for Driven piles in the state of Mississippi. Further, an examination of the setup potential after the piles have been installed to include within the resistance factors provide a potential cost effective design methodology that is specific to the soil conditions and pile material alternatives within the state. Based on the results of this study, it is recommended that the MDOT designers consider utilizing the LRFD resistance factors presented in Table 22, as well as utilizing the information presented in Tables 15 or 16 depending on the location and soil conditions encountered.

REFERENCES

[1] R. Skov and H. Denver, "Time-dependence of bearing capacity of piles," BiTech Publishers, Vancouver, Canada, 1988.

[2] B. J. Pement, "Evaluation of WBUZPILE design methodology and the development of a LRFD driven pile resistance factor for Alabama soils," The University of South Alabama, Mobile, 2017.

[3] R. Luna, "Evaluation of Pile Load Tests for use in Missouri LRFD Guidelines," Missouri Department of transportation, Jefferson City, 2014.

[4] J. DiMaggio, T. Saad, T. Allen, R. Barry, Al Dimillio, G. Goble , P. Passe, T. Shike and G. Person, "FHWA International Technology Exchange Program, report number FHWA-PL-99-013," FHWA, 1999.

[5] S. G. Paikowsky, B. Birgisson, M. McVay, T. Nguyen, C. Kuo, G. Beacher, B. Ayyub, K. Stenersen, K. O'Malley, L. Chernauskas and M. O'Neill, Load and Resistance Factor Design (LFRD) for deep foundations - NCHRP report 507, Washington D.C.: Transportation Research Board of The National Academies, 2004.

[6] M. A. Styler, "Development and implementation of the Diggs format to perform LRFD resistance factor calibration of driven concrete piles in Florida," University of Florida, Florida, 2006.

[7] M. N. Haque and Abu-Farsakh, "Estimation of Pile Setup and Incorporation of resistance factor in Load Resistance Factor Design Framework," ASCE, 2018.

[8] T. M. Allen, S. A. Nowak and R. J. Bathurst, "Calibration to Determine Load and Resistance factors for Geotechnical and Structural Design," Transport Research Board, Washington D.C., 2005.

[9] A. Vesic, Design of Pile Foundations, Washington D.C.: Transportation Research Board, 1977.

[10] Federal Highway Administration, "Design and Construction of Driven Pile Foundations - Lesson learned on the Central Artery/Tunnel Project," Georgetown Pike, 2006.

[11] B. Wrana, "Pile Load Capacity – Calculation Methods," *Studia Geotechnica et Mechanica,* Vols. Vol. 37, No. 4, 2015.

[12] E. J. Steward, J. Cleary, A. Gillis, R. Jones and E. Prado, "Investigation of Pile Setup (Freeze) in Alabama. Development of a Setup Prediction Method and Implementation into LRFD Driven Pile Design," University of South Alabama, Mobile, AL, 2015.

[13] Federal Highway Administration, "Load and Resistance Factor Design (LRFD) for HIghway Bridge Substructures," U.S. Department of transportation, 2001.

[14] AASHTO, "LRFD Bridge Design Specifications (7th edition)," American Association of State Highway and Transporation Officials, Washington D.C., 2014.

[15] K. Birid, "Evaluation of Ultimate Pile Compression Capacity from Static Pile Load Test Results," *1st GeoMEast International Congress and Exhibition,* pp. 1-14, 2017.

[16] Federal Highway Administration, "Geotechnical Engineering Circular No. 12 - Volume II: Design and Construction of Driven Pile Foundations," Washington DC, National Higghway Institute/ U.S. Department of Transportation, July, 2016.

[17] ASTM D1143-07, "Standard Test Methods for Deep Foundations Under Static Axial Compressive Load. Book of ASTM Standards," ASTM International, West Conshohocken,, 2014.

[18] S. S. AbdelSalam, S. Sritharan, M. T. Suleiman and M. Roling, "Development of LRFD Procedures for Bridge Pile Foundations in Iowa - Volume III: Recommended Resistance Factors with Consideration of Construction Control and Setup," Iowa State University, Ames, IA, 2012.

[19] P. J. Hannigan, F. Rausche, G. Likins, B. Robinson and M. Becker, Design and Construction of Driven Pile Foundations - Volumes I and II, Washington D.C.: Federal Highway Administration, 2016.

[20] D. P. Coduto, Foundation Design: Principles and Practices, Englewood Cliffs, NJ: Prentice-Hall Inc., 2001.

[21] S. Lanyi-Bennett and L. Deng, "Axial load testing of helical pile groups in glaciolacustrine clay," *Canadian Geotechnical Journal,* vol. 56, no. 2, pp. 187-197, 2019.

[22] E. A. Smith, "Pile-Driving Analysis by the Wave Equation, Journal of the Soil Mechanics and Foundation Division," ASCE, 1962.

[23] G. Likins, L. Liang and T. Hyatt, "Development of Automatic Signal Matching Procedure - iCAP," Proceedings from Testin and Design Methods for Deep Foundations, 2012.

[24] M. N. Haque and E. J. Steward, "Evaluation of Pile Setup Phenomenon for Driven Piles in Alabama," ALDOT and University of South Alabama, 2019.

[25] F. Rausche, G. Likins and H. Hussein M, "Analysis of post-installation dynamic load test data for capacity evaluation of deep foundations," Proc. from Research In Practice in Geotechnical Engineering (Geo-Concgres 2008), Lousiana, 2008.

[26] M. C. McVay, L. B. Birgisson, L. Zhang, A. Perez and S. Putcha , "Load and resistance factor desifn (LRFD) for driven piles using dynamic methods-A Florida Perspective," Geotechnial Testing Journal, 2000, 2000.

[27] J. H. Schmertmann, "The mechanical aging of soils," J. Geotech. Engineering Vol. 117 (9) pp. 1288-1330, 1991.

[28] L. Yang and R. Liang, "Incorporating setup into reliability-based design of driven piles in clay," Can. Geotech. Journal 43 (9): pp 946-955, 2006.

[29] A. S. Nowak and K. R. Collins, Reliability of Structures, Second Edition, Boca raton: CRC Press, 2007.

[30] D. A. Bostwick, "Calibration of Resistance Factos for Driven Piles using Static and Dynamic Test," University of Arkansas, Fayetteville, 2014.

[31] R. C. Patev, "Risk Technology Workshop: Engineering Reliability Concepts, Introduction to Engineering Reliability," United States Army Corps of Engineers, 2010.

[32] C. A. Cornell, "Structural safety specifications based on secondmoment reliability," Symposium Int. Association Bridges and Structural Engineering, London, 1969.

[33] N. C. Lind, "Consistent partial safety factors," Journal of Structural Engineering, 1971.

[34] K.-K. Phoon, F. H. Kulhawy and M. D. Grigoriu, "Development of a Reliability-Based Design Framework for Transmission Line Structure Foundations," Journal of Geotechnical and Geoenvironmental Engineering, ASCE, 2003.

[35] S. C. Reddy and A. W. Stuedlein, "Ultimate limit state reliability-based design of augered cast-in-place piles considering lower-bound capacities," Canadian Geotechnical Journa, NCR Research Press, 2017.

[36] AASHTO, "LRFD bridge design specifications, 3rd edition.," American Association of State Highway and Transportation Officials (AASHTO), Washington D.C., 2007.

[37] R. J. Bathurst, B. Q. Huang and T. M. Allen, "LRFD Calibration of steel reinforced soil walls," In Proceedings of Geo-Frontiers 2011, 2011.

[38] A. W. Stuedlein, W. J. Neely and T. M. Gurtowski, "Reliabilty-based design of augered cast-in-place in granular soils.," Journal of Geotechnical and Geoenvironmental Engineering., 2012.

[39] M. C. McVay, V. Alvarez, L. Zhang, A. Perez and A. Gibsen, "Estimating driven pile capacities during construction," 2002.

[40] J. Jabo, "Reliability-Basd Design and Acceptance Protocol for Driven Piles," University of Arkansas, Arkansas, May, 2014.

[41] E. J. Steward and J. Cleary, "CALIBRATION OF LRFD RESISTANCE FACTORS FOR DRIVEN PILES IN ALABAMA SOILS USING FOSM, FORM, AND MONTE CARLO SIMULATION METHOD.," Mobile, 2020.

[42] G. Likins, "Pile Testing - Selection and Economy of Safety Factors," 2004.

[43] S. Paikowsky and L. Chernauskas, "Energy approach for capacity evaluation of driven piles.," *Proceedings of Fourth International Conference on the Application of Stress-Wave Theory to Piles,* pp. 595-601, 1992.

[44] B. Widjaja, "Wave Equation Analysis and Pile Driving Analyzer For Driven Piles: 18th Floor Office Building Jakarta Case," *International Civil Engineering Conference Towards Sustainable Civil Engineering Practice Surabaya,* pp. 1-8, 2006.

[45] B. J. Pement, "Evaluation of WBUZPILE design methodology and the development of a LRFD driven pile resistance factor for Alabama soils," The University of South Alabama, Mobile, 2017.

[46] ASTM D4945-08., "Standard Test Method for High-Strain Dynamic Testing of Piles.," ASTM International, West Conshohocken, PA, 2008.

[47] AASHTO, "LRFD bridge design specifications, 3rd ed.," AASHTO, Washington D.C., 2004.

[48] L. Soderberg, "Consolidation theory applied to foundation pile time effects," *Geotechnique,* vol. 11, no. 3, p. 217–225, 1961.

[49] J. Pestana, C. Hunt and J. Bray, "Soil Deformation and Excess Pore Pressure Field around a Closed-Ended Pile," *Journal of Geotechnical and Geoenvironmental Engineering,* vol. 128, no. 1, 2002.

[50] V. Komurka, A. Wagner and T. Edil, "Estimating Soil/Pile Set-u," Wisconsin Highway Research Program, 2003.

[51] V. Sawant, S. Shukla, N. Sivakugan and B. Das, "Insight into pile set-up and load carrying capacity of driven piles," *International Journal of Geotechnical Engineering,* vol. 7, no. 1, pp. 71-83, 2013.

[52] M. Ashour, A. Helal and H. Ardalan, "Upgrade of Axially Loaded Pile-Soul Modeling with the implementation of LRFD Design procedure," University of Alabama, Huntsville, Huntsville, 2012.

[53] E. D. Prado Villegas., "Development of LRFD driven pile resistance factor by first order second moment method in Alabama soils," University of South Alabama, Mobile, AL, 2015.